Copyright Warning & Restrictions

The copyright law of the United States (Title 17, United States Code) governs the making of photocopies or other reproductions of copyrighted material.

Under certain conditions specified in the law, libraries and archives are authorized to furnish a photocopy or other reproduction. One of these specified conditions is that the photocopy or reproduction is not to be "used for any purpose other than private study, scholarship, or research." If a, user makes a request for, or later uses, a photocopy or reproduction for purposes in excess of "fair use" that user may be liable for copyright infringement,

This institution reserves the right to refuse to accept a copying order if, in its judgment, fulfillment of the order would involve violation of copyright law.

Please Note: The author retains the copyright while the New Jersey Institute of Technology reserves the right to distribute this thesis or dissertation

Printing note: If you do not wish to print this page, then select "Pages from: first page # to: last page #" on the print dialog screen

ABSTRACT

LOW PRESSURE CHEMICAL VAPOR DEPOSITION OF TUNGSTEN AS AN ABSORBER FOR X-RAY MASKS

by
Hongyu Chen

Tungsten film is one of promising materials for X-ray absorber in X-ray Lithography technology because of its high X-ray absorption and refractory properties. This study focus on CVD method to make tungsten film for X-ray absorber.

In this work, a cold wall, single wafer, Spectrum 211 CVD reactor was used for the deposition of tungsten from H_2 and WF_6. The growth kinetics were determined as a function of temperature, pressure and flow ratio. The deposition rate of as deposited tungsten films was found to follow an Arrehnius behavior in the range of 300-500°C with an activation energy of 55.7 kJ/mol. The growth rate was seen to increase linearly with total pressure and H_2 partial pressure. In the H_2/WF_6 ratio studies conducted at 500°C and 500mTorr, growth rate increase with flow ratio when lower than 10 followed by saturation above this ratio. The stress of as deposited film strongly dependent on deposition temperature and has weak relationship with pressure and flow ratio. The 'buried layer model' can explain the stress of as deposited film very well. The resistivity of the film is no relationship with pressure, flow ratio and dependent on temperature. The deposited films have preferred orientation of the (200) plane.

LOW PRESSURE CHEMICAL VAPOR DEPOSITION OF TUNGSTEN AS AN ABSORBER FOR X-RAY MASKS

by
Hongyu Chen

A Thesis
Submitted to the Faculty of
New Jersey Institute of Technology
in Partial Fulfillment of the Requirements for the Degree of
Master of Science in Engineering Science

Interdisciplinary Program in Materials Science and Engineering

October 1995

APPROVAL PAGE

LOW PRESSURE CHEMICAL VAPOR DEPOSITION OF TUNGSTEN AS AN ABSORBER FOR X-RAY MASKS

Hongyu Chen

Dr. Roland A. Levy, Thesis Advisor — Date
Professor of Physics,
Director of Materials Science and Engineering, NJIT

Dr. James M. Grow — Date
Professor of Chemical Engineering, Chemistry, and
Environmental Science, NJIT

Dr. Lev N.Krasnopetov — Date
Professor of Chemical Engineering, Chemistry, and
Environment Science, NJIT

BIOGRAPHICAL SKETCH

Author: Hongyu Chen

Degree: Master of Science in Engineering Science

Date: October 1995

Undergraduate and Graduate Education:

- Master of Science in Engineering Science,
  New Jersey Institute of Technology,
  Newark, New Jersey, 1995

- Master of Science in Polymer Science,
  East China University of Science and Technology,
  Shanghai, P.R. China, 1994

- Bachelor of Science in Chemical Engineering,
  Nanjing Institute of Chemical Technology,
  Nanjing, P.R.China, 1991

Major: Materials Science and Engineering

This thesis is dedicated to
my parents Chaozi Chen and Yulan Ding

ACKNOWLEDGMENT

The author wishes to express his sincere gratitude to his advisors, Professor Roland A. Levy for his guidance, friendship, moral and financial support throughout this thesis work, without which it would not have been completed. Special thanks to Professor James M.Grow and Lev N.Krasnoperov for serving as member of the committee.

The author appreciates the timely help and suggestions from the CVD Lab. members, including: Mahalingam Bhaskaran, Jan Opyrchal, Lan Chen, Manish Narayan, Emmanuel Ramos and especially to Vitaly Sigal for his invaluable technical assistance, co-worker David Perese who provided assistance on all aspects of this project, Chenna Ravindranath and Majda Newman who provided the X-ray diffraction data.

TABLE OF CONTENTS

TABLE OF CONTENTS
(Continued)

Chapter **Page**

TABLE OF CONTENTS
(Continued)

LIST OF TABLES

LIST OF FIGURES

LIST OF FIGURES
(Continued)

CHAPTER 1

INTRODUCTION

1.1 Tungsten-One of the Most Desirable X-ray Absorbers

X-ray lithography is a promising technique for replicating sub-micron patterns of large area[1]. One of the key factors in X-ray lithography is the construction of the mask. This is because the resolution and accuracy of X-ray lithography is determined by the X-ray mask. The mask essentially consists of absorber patterns and a thin mask substrate. Among many absorbers, tungsten is the most promising material not only because of its high X-ray absorption, but also because of its low thermal expansion, high Young's modules and its refractory properties. However, it is difficult to control the stress in the tungsten film. This study focuses on chemical vapor deposition of low stress tungsten film. In this chapter, the importance of X-ray mask for X-ray lithography is presented. Then low stress in X-ray absorber is justified followed by a discussion of the general concepts of CVD (Chemical Vapor Deposition). Finally, a systematic review of the development of CVD tungsten is presented.

1.1.1 The Promising Application of X-ray Lithography

Lithography is one of the most important technologies in the mass production of microelectronic circuits[2]. More is spent for lithographic systems than for any other type of IC processing equipment in a production line. Lithography has allowed the

devices, which have been reshaping our world for 30 years. The trend towards smaller-feature size devices will not stop until some fundamental limit is encountered in device operation, or fabrication costs increase radically with the reduction in feature size. Optical lithography has made great strides in providing smaller and smaller structures, but it presently appears that the practical resolution limit using near-U.V. coherent sources is larger than 0.3 μm. This limit is determined by diffraction effects and practical limits on lens systems. To permit the transition to smaller details some methods have been developed that use electrons or ions instead of light. The effective wavelength of these particles is much smaller than the dimensions of the details required, so that diffraction effects are no longer a problem. Another promising method for VLSI is X-ray lithography, in which X-rays are used to produce an image of the mask pattern on a slice coated with X-ray sensitive resist. The wavelength of the radiation varies from about 0.5 to 3nm, so that no diffraction effects occur. As compared with the electron method, X-ray lithography at these wavelengths has the advantage that there is no proximity effect[3].

1.1.2 X-ray Mask

The major effort in X-ray lithography is focused on the development of an appropriate mask technology. Considering the progress in all other elements of X-ray lithography, the successful industrial application of this new technology will depend primarily on whether the remaining problems in mask technology can be solved. The X-ray mask consists of a thin membrane of low-Z material carrying a high-Z absorber pattern[4]. The requirements

for X-ray mask quality are rigid and cannot be compromised. For the membrane material, such requirements include[5]:

- high X-ray transmission (>80% at 0.4-1.5nm)
- adequate optical transmission (>60% at 633nm)
- high modules of elasticity ($>10^{11}$Pa)
- low stress ($<5\times10^{8}$ dynes cm^{-2})
- low defect density ($0.1cm^{-2}$)
- long lifetime ($>10^{6}$ exposures at a flux of 100mw cm^{-2})
- flatness (<0.3μm)
- radiation hardness (<10nm distortions at absorbed does $>10^{3}$ kJ cm^{-3})
- low cost ($5,000)

For the absorber, such requirements include:

- high x-ray absorption (>99% at 0.4-1.5 nm)
- low stress ($<5\times10^{8}$ dynes cm^{-2})
- low defect density (<0.1 cm^{-2})
- minimal feature distortion (<50 nm)
- ease of pattern

Among the numerous X-ray mask membranes considered, four have emerged as most promising. These are silicon, silicon nitride, silicon carbide and boron nitride. Silicon, a more versatile material, has been used with both Au and W as the absorber material[6]. In this study W was deposited on the Si wafer which is a promising membrane material and is easily available.

In X-ray lithography, pattern features on the mask should not deviate from their assigned in-plane positions by more than a fraction of the minimum line width. In an X-ray lithography mask, such distortion can arise if the absorber, which is in relief on the mask membrane, has non zero internal stress. Absorber stress exerts a torque on the membrane at the edges of features, and this leads to out-of-plane and in plane distortion. Therefore, to reduce distortion to acceptable levels one must achieve near-zero internal stress [7]. Since the X-ray lithography was first developed, Au(gold) has been used as an X-ray mask absorber. This is because that the Au has a high absorption coefficient, and the internal stress of Au film can be easily controlled by selecting the deposition condition. However, it is known that the stress in gold changes with time, even at room temperature[8]. Moreover, Au cannot be dry etched and its thermal expansion coefficient ($14.2\times10^{-6}\,K^{-1}$) is much larger than that of mask membranes such as Si ($2.6\times10^{-6}\,K^{-1}$) and SiC ($3.8\text{-}4.2\times10^{-6}\,K^{-1}$). Tungsten (W) is an attractive alternative to Au because it is refractory, can be dry etched in fluorine-containing gases and has a much lower thermal expansion coefficient ($4.5\times10^{-6}\,K^{-1}$) than gold[9]. Moreover, it absorbers more effectively than gold(and may further reduce the aspect ratio requirements). However, there are several problems associated with W: (1) its internal stress is a strong function of deposition parameters and hence achieving zero stress can be problematic [10]; (2) there is a metastable phase of W, β-W, which can be incorporated in deposited films. The β-W can transform to the stable phase α-W and, in the process, change the net stress[11] , and (3) the high electron backtering from W may increase the difficulty of pattering.

1.1.3 The Development of Low Stress Tungsten Film

1.1.3.1 Kinds of Stress in the Thin Film: The total stress in a film is the sum of: (a) the thermal stress, resulting from the difference in the coefficient of thermal expansion between the film and the substrate; (b) the intrinsic stress, which originates from the change in the film structure.

The thermal stress caused by the difference in thermal expansion coefficients (α) between film and substrate. After cooling from deposition temperature (T) to room temperature (T_o), the biaxial thermal stress(σ_{th}) in a film on a substrate is obtained from

$$\sigma_{th} = \frac{Ef}{1-\nu f}\int_{To}^{T} \Delta\alpha\,(T')dT \qquad (1.1)$$

where E_f is young's modules and ν_f is the Poisson constant of the film. For the case of tungsten film, E_f =410 GPa and ν_f=0.28. Since the average linear thermal expansion coefficients between 20 and 500°C for W and SiC amount to 4.6 and 4.2×10^{-6} K^{-1} respectively, the thermal stress due to cooling is only $0.23\times\Delta T$. The thermal stress is very small, the high residual stress values are ascribed to intrinsic stress.

The stress present in the absence of thermal effects are usually called intrinsic stresses or, more appropriately, growth stress. Such stresses are associated with the growth of a film on a substrate.

1.1.3.2 Low Stress Tungsten Film by PVD: In literature of tungsten film for X-ray absorber application deposition by PVD prevails. However,tungsten films deposited by PVD (i.e.,sputtering, evaporation) have large stress. To reduce the stress in the PVD tungsten film, some methods were suggested, which include:

(1) Ion implantation

Yao C, et al.[12] reduce the stress in tungsten film by using Si ion implantation to a projected range of 10nm in the W at does in the range of 10^{15}-10^{16} cm^{-2}. Distortion correction takes place because the implantation produces compressive stress near the upper surface, resulting in a torque that balances a torque of opposite sign at the absorber-membrane interface due to tensile stress in the tungsten.

H. Luethje et al. [13] reported effective stress reduction ($\sigma<10^7$ N/m^2) and excellent long term stability ($\Delta\sigma<5\times10^6$ N/m^2) are being obtained by sputtering the 0.8 μm thick tungsten layers in the presence of oxygen, and subsequently annealing them in an oxidizing atmosphere.

(2)Tungsten alloy

Yoshioka, et al. [14] investigated W-Ti alloy as x-ray mask absorber. The W-Ti film were deposited by sputtering the W-Ti (1 wt% Ti content) target using $Ar+N_2$ gas with a DC magnetron sputtering system. They obtained the low stress tungsten film which is satisfactory for an X-ray mask absorber.

1.1.3.3 Low Stress Tungsten Film by CVD: There are reports about low stress tungsten film by CVD for interconnect or plug application in VLSI technology. Up to now, no

report about W CVD film for X-ray absorber application was found. In a later review of CVD tungsten, we will discuss low stress W film by CVD.

1.2 Chemical Vapor Deposition

Chemical vapor deposition(CVD) is one of the most important methods of film formation used in the fabrication of very large scale integrated (VLSI) silicon circuits, as well as of microelectronic solid state devices in general. In this process, chemicals in the gas or vapor phase are reacted at the surface of a substrate where they form a solid product[15].

1.2.1 Basic Steps of CVD

A CVD process basically is a type of surface catalysis process since the deposition process is thermodynamically favorable and takes place on the substrate surface. Most of the time the surface serve as a catalyst for the reactions leading to amorphous deposition and crystal growth. The same sequence of events in a heterogeneous reaction can therefore be applied to crystal growth by CVD[16] . These events are:

(a) a given composition (and flow rate) of reactant gases and diluent inert gases is introduced into a reaction chamber.

(b) then gaseous species diffuse to the substrate.

(c) the reactants are adsorbed on the substrate.

(d) the adsorbed reactants undergo migration and film forming chemical reactions.

(e) the gaseous by-products of the reaction are desorbed.

(f) gaseous transport of by-products.

(g) bulk transport of by-products out of reaction chamber.

1.2.2 Experimental Parameters in CVD

Any one of the several steps taking place in a CVD process can be the rate-determining step. A number of experimental parameters play an important role in determining or altering the rate-determining step. The experimental parameters, which are discussed individually below are: deposition temperature, reactant partial pressure, gas flow rate.

1.2.2.1 Deposition Temperature: The rate of product deposition is dependent primarily on temperature. The rate controlling step in the process such as surface reaction, and surface diffusion can be described by the Arrhenius equation.

$$R=R_o\exp(-E_a/kT) \qquad (1.2)$$

Activation energy signifies the presence of an energy barrier which must be overcome in order for the process to occur. Activation energies for most surface processes are usually greater than 10 kcal/mole and lie in the range of 25-100 kcal/mol[16]. Conversely, mass transport phenomena such as diffusion are almost insensitive to temperature. Therefore, when plotted as an Arrhenius expression (the deposition rate vs the reciprocal temperature) to find activation energies, a preliminary distinction between

the surface phenomena and the gas phase mass transport phenomena can be made by observing the temperature dependence of the process.

A typical Arrhenius plot exhibits two regions as shown in figure 1.1. At lower temperature, there is always enough supply of reactants to the surface and this supply is faster than the consumption of the reactants during reaction. Then the overall rate is controlled by the surface kinetics. At higher temperature, the rate is limited by the rate of

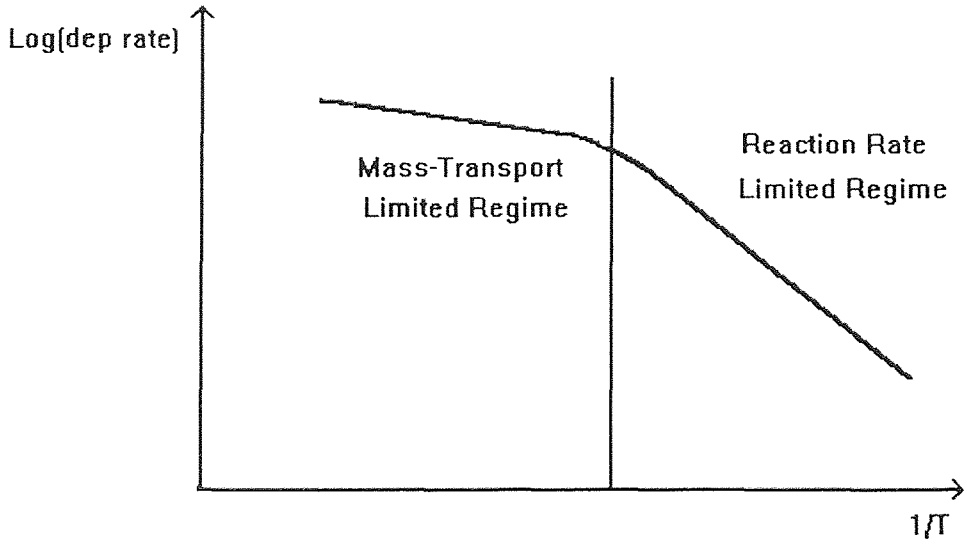

Figure 1.1 Temperature dependence of growth rate for CVD films

insufficient reactants supply although the rate of surface reaction is higher. It is possible to switch from one rate limiting step to the other by changing the temperature as shown in figure 1.1 [17].

Thermodynamic aspects of the reaction system should also be considered when examining the effect of deposition temperature. Assuming the process is near equilibrium,

the temperature effect on deposition based on the thermodynamic considerations is presented in Table 1:

Table 1. Temperature effect on reaction by thermodynamic consideration

From Van't Hoff's Equation $d \ln Kp/dT=\Delta H/RT^2$ If $\Delta H>0$ and T is increasing a. Kp increases b. Reaction shifts to right c. Deposit product increases e. A cold wall reactor with rf-heated substrate is needed

1.2.2.2 Gas Pressure: Surface reactions involving single adsorbed molecules are classified as unimolecular reaction[18].This can be treated by Langmuir adsorption isotherm. Let θ be the fraction of surface that is covered and $1-\theta$ the fraction that is bare. The rate of adsorption is then $k_1P(1-\theta)$, where P is the gas pressure and k_1 is proportionality constant. The rate of desorption is $k_{-1}\theta$. At equilibrium, the rates of adsorption and desorption are equal, so that

$$\frac{\theta}{1-\theta} = \frac{k_1}{k_{-1}} P = KP \qquad (1.3)$$

where K, equal; to k_1 / k_{-1}, is the adsorption equilibrium constant. The equation can be written as

$$\theta = \frac{KP}{1+KP} \tag{1.4}$$

The rate of reaction is proportional to θ and may therefore be written as

$$D.R = k_2\theta = \frac{k_2 KP}{1+KP} = k_o \cdot e^{\frac{-Ea}{RT}} \frac{KP}{1+KP} \tag{1.5}$$

where k_o is the proportionality constant at certain temperature. This is the simplest treatment of surface reaction.

1.2.2.3 Gas Flow Rate: When growth rate for a CVD process is plotted as a function of reactant gas flow rate, the generalized form of the relationship is shown in figure 1.2 [19]. At very small flow rate (region 1), the incoming gas stream has sufficient residence time to equilibrium with the substrate surface. Increasing the total flow rate increases the rate of reactant input, and thus more material per unit time equilibrates with the substrate surface. The rate increases linearly with total flow rate in this region[20].

When the flow rate is increased above a certain point, the entire gas stream no longer has sufficient residence time for complete equilibrium (region 2). At this point, a portion of the incoming reactants pass by unreacted. This gives higher bulk stream partial

pressures than the surface partial pressure. Then the rate-limiting process is diffusion from the main gas stream to the substrate surface. It is known that the boundary layer thickness, where the diffusion process takes place, is inversely proportional to the square root of the gas velocity[21]. Then, in this regime, the surface reaction shows a square root dependence on the gas flow rate.

At high flow rate, the reaction rate reaches a plateau (region III) and becomes independent of flow rate[22]. Here the reaction rates are so slow relative to the gas flow and mass transfer rates that the partial pressure at the surface becomes essentially the input partial pressure. Then the process is said to be 'kinetically controlled'. The reactant flow rate for kinetics studies should be in this plateau regime so that the true temperature and partial pressure dependence of the reaction can be observed.

1.2.3 Types of CVD Processes

1.2.3.1 Classification of Process Types: CVD processes can be classified according to the type of energy supplied to initiate and sustain the reaction: (i) Thermally activated reactions at various pressure ranges, which comprise the vast majority of CVD processes; heat is applied by resistance heating, rf induction heating, or infrared radiation heating techniques. (ii) Plasma promoted reactions, where an rf (or dc)-induced glow discharge is the source for most of the energy that initiates and enhances the rate of reaction. (iii) Photon induced reactions, where a specific wavelength radiation triggers and sustains the reaction by direct photolysis or by an energy transfer agent, such as uv-activated mercury.

1.2.3.2 Thermally Activated Atmospheric Pressure Processes (APCVD): The simplest CVD process type is conventional atmospheric or normal pressure CVD

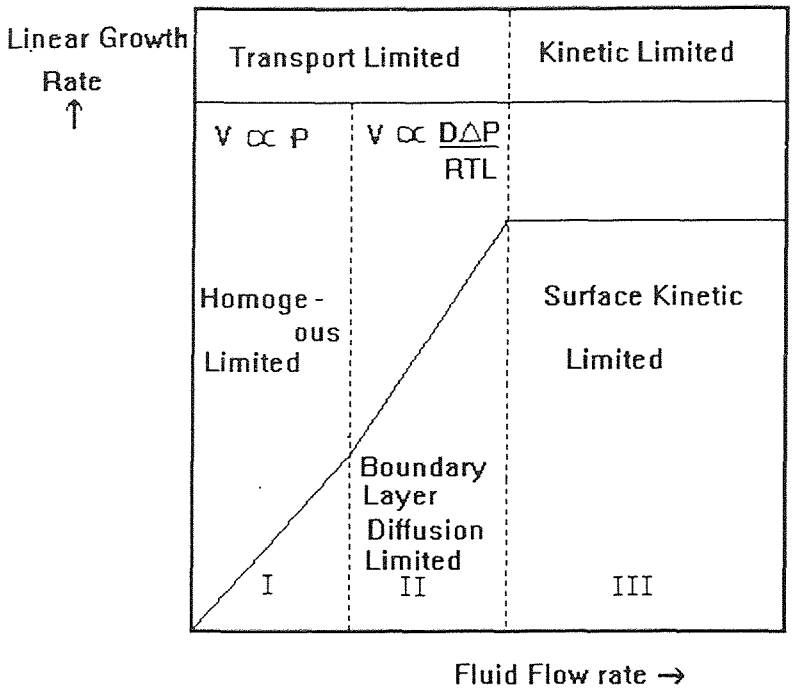

Figure 1.2 Idealized growth-rate versus fluid flow-rate plot showing the different growth regimes

(APCVD or NPCVD)[23]. Reactant vapors or gases are introduced in the reactor at normal atmospheric pressure. The pressure in the reactor system is slightly above atmospheric due to the impedance of the gas flow at the exit part of the system. The temperature and reactant flow rate determine the rate of film deposition. Heat is supplied by resistance heating, by rf induction techniques, or by infrared radiation. The advantage of APCVD is its simplicity; no vacuum pumps are needed. The disadvantage is the

tendency for homogeneous gas phase nucleation that leads to particle contamination, unless special optimized gas injection techniques are used.

1.2.3.3 Thermally Activated Low Pressure Processes (LPCVD): Low pressure CVD is widely used in the extremely cost competitive semiconductor industry for deposition films of insulators, amorphous and polycrystalline silicon, refractory metals, and silicides[24]. The gas pressure of ~0.5 to 1 Torr employed in LPCVD reactors distinguishes it from conventional CVD systems operating at 760 Torr. Lowering the gas pressure enhances the mass transfer rate relative to the surface reaction rate. The mass transfer of gases involves their diffusion across a slowly moving boundary layer adjacent to the substrate surface. The thinner this boundary layer and the higher the gas diffusion rate, the greater the mass transport that results. Although the boundary layer for LPCVD is thicker than that of APCVD, the diffusivity (D) for LPCVD is much higher than APCVD, thus, low pressure deposition conditions enhance mass transfer greatly, providing high wafer capacity, better thickness uniformity and less gas phase reactions, which are especially important in VLSI processing where a very high device reliability and high product yield must be achieved[25]. The disadvantages are the relatively high operation temperature.

1.2.3.4 Plasma- Enhanced Deposition Processes (PECVD): Plasma deposition[26] is a combination of a glow discharge process and low pressure chemical vapor deposition in which highly reactive chemical species are generated from gaseous reactants by a glow discharge and interact to form a thin solid film product on the substrate. Since plasma

causes the breakdown of the gas molecule into a variety of very reactive species, PECVD is carried out at substrate temperatures lower than those of APCVD and LPCVD process[27]. The radicals formed in the plasma discharge have high sticking coefficients and upon adsorption they can migrate easily on the surface to yield conformal structures. Film with low pinhole density and with good adhesion to the substrate can be deposited with this method. Concerning disadvantages of PECVD, the complexity of reactions make the synthesis of stoichiometric compositions difficult. A consequence of the low temperature of film formation, by-products are trapped in the films, which cause problems in later stages of manufacturing MOS circuits.

1.2.3.5 Photo-Enhanced Chemical Vapor Deposition (PHCVD): This type of process is based on activation of the reactants in the gas or vapor phase by electromagnetic (usually short wave ultraviolet) radiation[28,29]. Selective absorption of photonic energy by the reactant molecules or atoms initiates the process by forming very reactive free radical species that interact to form a desired film product. The advantages of this promising CVD process is the low temperature needed to form films and the greatly reduced radiation damage (compared to PECVD) that results. The limitations is the need for photoactivation with mercury to achieve acceptable rates of film deposition.

1.2.3.6 Laser-Enhanced Chemical Vapor Deposition (LCVD): Chemical vapor deposition involving the use of lasers can be categorized in two types of processes[30]: (1) pyrolysis (2) photolysis. In pyrolysis process the laser heats the substrate to decompose

gases above it and enhance rates of chemical reactions there. Photolysis, on the other hand, involve direct dissociation of molecules by energetic photons. Among several advantages of these techniques are spatial resolution that can be achieved and the ability to interface with laser annealing, diffusion, and localized heat treatments, but LCVD is still in its early development.

1.3 Chemical Vapor Deposition of Tungsten

1.3.1 Tungsten Film Application

The semiconductor industry is experiencing rapid technological growth in the area of submicron IC device fabrication which has lead to continually shrinking device feature size. Performance and reliability concerns for these approaches have lead to consideration of low resistivity material, such as tungsten. In fact, tungsten applications at production level have already started. Tungsten provides low resistance (5.6μΩ-cm of bulk resistivity), low stress ($<5\times10^9$ dyne/cm^2), excellent conformal step coverage and a thermal expansion coefficient which is close to that of silicon. Another important feature for tungsten is its high resistance to electromigration, while in the current technology aluminum severely suffers from it [31].

There are two aspects of tungsten CVD for integrated circuits that have taken on commercial importance. One is the blanket deposition or nonselective deposition, in which deposition proceeds uniformly over variety of surfaces. A primary application of blanket W CVD is for interconnects, which is shown schematically in figure 1.3. Another application for blanket W CVD is via hole filling to planarize each level for subsequent

processing. This is achieved by depositing a conformal film and etching back to the insulator surface (figure 1.3.). The second area of interest is the "selective" CVD of tungsten, where deposition occurs on silicon but not on silicon dioxide. Here one can selectively fill via holes to either provide a thin barrier metal or to deposit a thicker to help planarize the circuit. Both applications involve processing step, and are attractive for this reason [32].

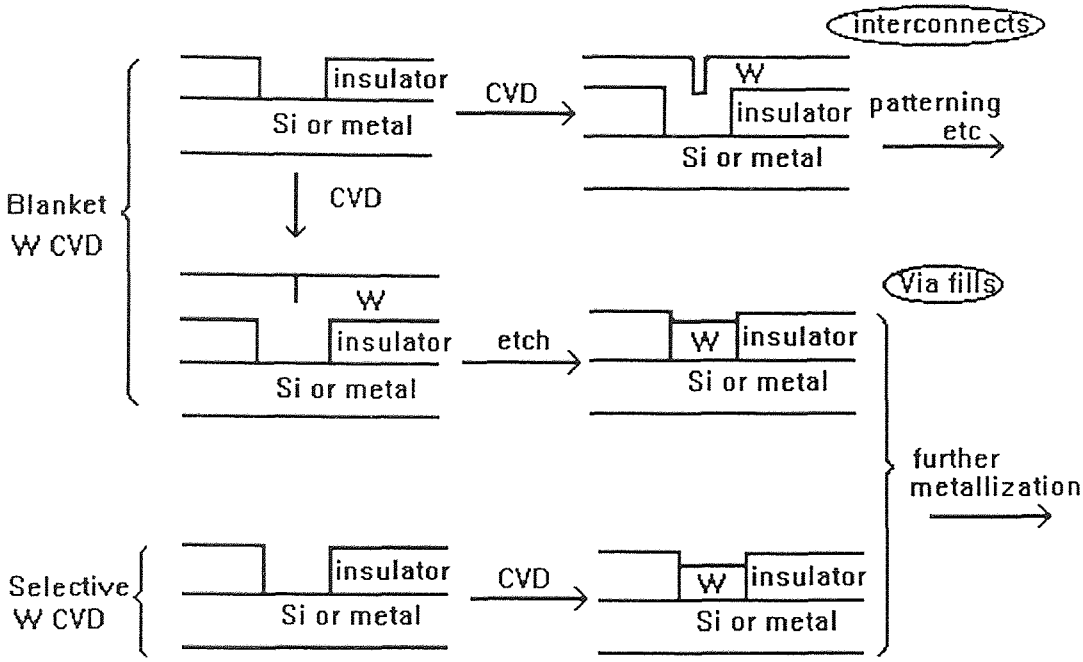

Figure 1.3 Schematic for applications of blanket and selective metal CVD for microelectronics applications

1.3.2 Reaction for CVD of Tungsten

Tungsten can be chemically vapor deposited by reduction of WF_6 or WCl_6. The common reductant are silicon (Si), hydrogen(H_2), silane (SiH_4). Only a few studies were done on

WCl_6 as the source of tungsten. Because W films deposited from WF_6 have an advantage over hose deposited from WCl_6 in that lower contact resistance to Si may be achieved. Furthermore, WF_6 is a liquid that boils at room temperature, whereas WCl_6 is a solid that melts at 275°C, making its use as a CVD source more difficult[33]. Tungsten also can be deposited by the pyrolysis of $W(CO)_6$, the weaker W-CO bonds (CO is a neutral ligand) allow for unimolecular dissociation at low temperature, but the deposition of W from $W(CO)_6$ does not exhibit selectivity [34].

The free energy change ΔG for WF_6 reaction at 600 K are given in Table 2 [35]. Comparing these free energies, the free energy of Si reduction is more negative than that of H_2 reduction. So when the H_2 reduction reaction is carried out, it is the Si substrate that first react with WF_6. The substrate consumption will result encroachment, tunneling, creep-up and loss of selectivity problems[31]. After a certain W film thickness is reached this reaction will stop because the W film forms a diffusion barrier between the Si and WF_6 and prevents further reaction. This phenomenon is called self-limiting[36]. The SiH_4 reduction reaction is more favorable than the Si and H_2 reduction reactions. This reaction can suppress the Si reduction and Si consumption. Higher deposition rates at relatively lower temperatures and smoother resulting W/Si interfaces make this reaction very attractive. Recent developments of CVD tungsten have focused on this reaction.

1.3.2.1 Reduction WF_6 with Si: The reduction of WF_6 by solid silicon is of interest because of the potential of selective tungsten CVD for via hole filling for multilevel interconnect technology. This reaction is important because it is necessary to deposit some

tungsten before the normal reduction processes, i.e., WF_6+H_2 or SiH_4., can proceed. However, excessive consumption of silicon and other detrimental effects such as "wormhole" formation have limited the utility of this reaction.

Table 2 Free Energy Changes at 600 K

Reactions	ΔG, kcal/mol (based on 1 mole WF_6)
(A) $WF_6 + 1.5Si \rightarrow W + 1.5SiF_4$	-179.4
(B) $WF_6 + 3H_2 \rightarrow W + 6HF$	-27.9
(C) $WF_6 + 1.5\ SiH_4 \rightarrow W + 1.5SiF_4 + 3H_2$	-208.7
(D) $WF_6 + 2.1SiH_4 \rightarrow 0.2W_5Si_3 + 1.5SiF_4 + 4.2H_2$	-227.6
(E) $WF_6 + 3.5SiH_4 \rightarrow WSi_2 + 1.5SiF_4 + 7H_2$	-268.9

Fortunately, from a processing point of view, the Si +WF_6 reaction has often been found to be "self-limiting" and typically only 100 to 200Å of tungsten is deposited. The reaction is also very fast and reaches the self-limited thickness in a few seconds at typical LPCVD conditions. For the results of Broadbent and coworkers [37]the self-limiting thickness is deposited in 6 s and no additional deposition occurs for the time up to 6000s. Despite a lot of effort, the mechanism leading to self-limiting deposition is still not completely understood. One theory is that once a continuous tungsten film is formed the reaction slows down dramatically or shuts off completely because it becomes limited by

transport of one of the reactants to the active interface. One difficulty with this idea is that some self-limiting films appear to be very porous, although others have near bulk tungsten densities. Another theory [38] is that a "blocking" agent, namely, WF_4, builds up on the tungsten surface and inhibits deposition.

Green, et al.[39] examined the morphology of Si-reduced W films deposited between 210 and 700°C. The grains were spongy in structure, and the space is occupied by trapped gases and pores. Therefore, the film density was far less than tungsten bulk density.

Auger depth analysis showed that most of the oxygen in the W film is present at the Si/W interface[40]. Joshi,et al. [41] found 22-25% oxygen in the films deposited below 600°C, causing high film resistivities (130-140 μΩ-cm). The oxygen level drops to 12-14% at higher temperatures resulting in lower resistivities (60-70 μΩ-cm). A native oxide layer on the silicon surface was reported to be incorporated into the W films[42].

1.3.2.2 Reduction WF_6 with H_2: It was found that the H_2+WF_6 CVD process could be selective in that deposition occurred rapidly on many metals and semiconductors, but not on insulators such as SiO_2. Selectivity apparently occurs because deposition requires that the substrate be capable of either reducing WF_6 to metallic W, or dissociatively chemisorbing H_2 and WF_6. Most oxides do not readily support either of these processes and therefore tungsten deposition does not readily occur. The selective nature of the deposition process created much interest in that it significantly reduced the number of steps in the metallization process.

There have been numerous experimental kinetic studies covering LPCVD and APCVD conditions over a wide temperature range. Creighton, et al. [32] categorized them into two regimes. The first reaction regime described as being dominated by homogeneous reactions obeyed the following pressure dependence

$$\text{Rate} \propto P(WF_6)^2 \cdot P(H_2)^2 \qquad (1.6)$$

The conditions that lead to this kinetic regime generally have not been studied further. In another regime the reaction proceeded heterogeneously with the following pressure dependence

$$\text{Rate} \propto P(WF_6)^0 \cdot P(H_2)^{1/2} \qquad (1.7)$$

and an apparent activation energy of ~66.24 kJ/mol. The form of the rate law above has been verified by numerous workers for LPCVD conditions[43,44]. The phenomenon that the deposition rate depends on the H_2 flow rate, not on WF_6 rate suggests that surface-adsorbed H_2 dissociation is the rate-controlled mechanism.

Selective deposition of W on Si surfaces constitutes another area of concern in the H_2-reduction reaction. Joshi, et al. [45] have found that the selectivity of tungsten produced by silicon reduction is almost 100% while that by H_2 reduction depends on the prior condition of the Si wafer. McConica and Krishnamani [43] observed that the selectivity loss to silicon surfaces occurs at temperature higher than 300°C. The

temperature dependence suggested that the tungsten nucleation on the oxide is an activated process. In an ultra high vacuum (UHV) analysis chamber, Creighton[46] performed Auger electron spectroscopy and temperature programmed desorption studies on the selectivity loss. He suggested that a tungsten subfluoride desorption-disproportionation mechanism is the origin of transport of tungsten from the tungsten surface to the silicon dioxide surface. Tungsten pentafluoride, WF_5, was the best candidate to initiate the selectivity loss because of its volatility.

Studies of the CVD tungsten film morphology and impurity content are essential for the film quality, and thereby the film resistivity. Shroff and Delval [47] have measured the fluorine content of W films with photon activation analysis. The deposition of low fluorine content films was possible at high temperature, high H_2/WF_6 ratios and low pressures. Initial tungsten layers always started with a fine grain structure on the base metal substrates and continued to grow as elongated crystals. It was also reported that increasing H_2/WF_6 ratios and higher pressures resulted in less adherent and inhomogeneous coatings. This was exacerbated at high temperature due to nucleation in the vapor phase.

R.A.Levy[48], et al. observed wormhole formation in the Si substrate. They also reported that the wormhole is non-crystal resulting from both Si anh H_2 reduction of WF_6. McLaury[49], et al. have found that flourine was a major contaminant in the films. Transmission electron microscopy studies revealed damage at the (100) Si/SiO_2 interface in the form of worm tracks. Stacy[50], et al. performed TEM analyses on the W films and confirmed tungsten deposition filaments (also called wormholes or tunnels) in the silicon

substrate. Joshi[45], et al stated that H_2 reduction produces purer films than Si reduction by getting oxygen in the reaction chamber. Thus, the resistivities for H_2 reduced films (9-10$\mu\Omega$ -cm) are far less than those of Si reduced films (130-140 $\mu\Omega$-cm). They also noted that hydrogen reduction produces very rough films compared to silicon reduction.

The frequently observed preferential tungsten crystal orientation in the H_2 reduction reaction is W(100)[47]. High H_2/WF_6 ratios have been reported to give W(111) orientation[51]. In a more detailed structural study, Kamins[52], et al. examined orientation change with thickness for W films. They used a chromium nucleation layer to prevent the Si-WF_6 reaction from influencing the W film structure.

R.V.Joshi[53] found W film stress deposited from H_2 reduction is a strong function of temperature and a weak function of H_2/WF_6 ratio and pressure. High temperature, pressure, and H_2/WF_6 favor lower W film stress. The higher temperature, the lower stress. Other researchers[54] reported similar trend of stress dependency on temperature and H_2/WF_6 ratio and found the tensile to compressive stress conversion at chuck temperature of 500-700°C for a pressure of 1.5 Torr.

1.3.2.3 Reduction WF_6 with SiH_4: In addition to H_2 the reduction of WF_6 may be accomplished by a number of reducing gases and the most important alternative to H_2 is silane (SiH_4). SiH_4 is known to readily dissociatively chemisorb on clean tungsten surfaces. This tungsten CVD process via silane reduction is similar to the tungsten silicide CVD process that uses higher SiH_4/WF_6 pressure ratios and usually deposits in a nonselectively fashion[55]. For low SiH_4/WF_6 ratios (typically less than 1:1) the process

leads to α-W deposition, often with a high degree of selectivity. At somewhat higher SiH_4/WF_6 ratios (typically 1 to 3) the process leads to higher resistivity deposits of β-W or tungsten silicides, usually in a nonselective fashion. Some of the original work using silane as a reductant was actually aimed at preventing excess silicon substrate consumption or other detrimental interactions of WF_6 ($+H_2$) with the substrate such as encroachment or "wormhole" formation. In addition to the demonstrated selectivity and minimized silicon substrate damage, the process also generated interest because of the extremely high growth rates that could be achieved at relatively low temperature (up to ~1μm/min at 300°C). Some of the original enthusiasm has dampened as many workers found selectively difficult to maintain on a reliable basis, as was the case with the hydrogen reduction process.

Most of the kinetic studies [56]of the silane reduction process have been performed in LPCVD reactors. A weaker temperature dependence and the pressure dependence are generally observed:

$$Rate \propto P(WF_6)^n P(SiH_4)^1 \text{, n typically ~0 or slightly negative} \qquad (1.8)$$

The higher deposition rates and weak temperature dependence led a number of workers to suspect that the deposition process was mass transport limited.

Kobayashi[57], et al. used *in situ* infrared spectroscopy to sample the gas phase above a wafer in an LPCVD reactor during deposition. They found no evidence for HF production at typical CVD temperatures (250 to 350°C) but found that $SiHF_3$ rather than

SiF_4 was the main silicon fluoride produced, so they proposed the possible reaction pathway as follows:

$$WF_6(g)+2SiH_4(g)\rightarrow W(s)+2SiHF_3(g)+3H_2(g) \qquad (1.9)$$

The resistivity of tungsten deposited from silane reduction is related to the impurity content. Juugd[58], at al. employed AES and electron probe micro analysis to elucidate resistivity dependence on the incorporated silicon. On the contrary, Suzuki[59], et al. stated that resistivity depends mostly on fluorine content, as determined by SIMS analysis, rather than silicon and oxygen content. The film from SiH_4 reduction has higher resistivity value than that from H_2. S.Sivaram[60], et al. found not only the impurity content but also the microstructure account for this difference.

Orientation of deposited films is another factor to be considered for kinetic evaluations. X-ray diffraction patterns in some research papers showed a (110) preferred orientation of tungsten crystals when α-W was the dominant phase[35,55,59]. In contradiction to these, Schmitz[61],et al. reported a dominant (100) orientation for both H_2-WF_6 and SiH_4-WF_6 systems. These distinction may be a result of different deposition kinetics and/or be the different substrates.

The film deposited from silane reduction has higher stress than that from H_2 reduction[62]. Takayuki[63], et al. found different types of heating lead to different stress in the W film deposited from SiH_4 reduction. In IR-heating from the wafer back and in resistance heating, stress is tensile stress at low deposition temperature. The tensile stress

decreases as deposition temperature increases. In IR-heating from the wafer front, stress is compressive at all deposition temperature. Takashi[64], et al. use ECR plasma CVD system to deposit W film which has a low compressive stress due to ion bombardment.

1.3.2.4 Dissociation of $W(CO)_6$: Tungsten hexacarbonyl, $W(CO)_6$, is a stable solid with a relatively low vapor pressure (350 mTorr at 500 °C). Because the W-CO bond energy is relatively weak (~43 kcal/mol) compared with the W-F bond energy (~121 kcal/mol). This allows for tungsten deposition at relatively low temperatures without the aid of a reducing agent. Factors that have limited the utility of $W(CO)_6$ are the inconvenience of using a solid source, its low vapor pressure, and the incorporation of carbon and oxygen into the deposits.

Relatively clean α-W can be deposited bove 450°C at a rate of ~100Å/min and with resistivities 3 to 6 times the bulk value. Films deposited below 450°C are normally heavily contaminated with carbon, resulting in resistivities 20-300 times the bulk value, and exhibit an fcc crystal structure.The deposition rate exhibited an apparent activation energy of 18 kcal/mol[32].

Tungsten deposition via $W(CO)_6$ decomposition is nonselective toward Si and SiO_2. Films deposited on silicon oxides are generally adherent, in contrast to the hydrogen reduced WF_6 films. The hexacarbonal process does not produce the deleterious effects at the silicon interface that are sometimes seen with the hexafluoride processes. This is not surprising because CO interactions with silicon are rather weak and do not lead to gas-phase products.

CHAPTER 2

THE DEPOSITION PROCESS OF TUNGSTEN FILM

2.1 Reaction System

2.1.1 Equipment Set up

The deposition reaction was carried out in a SPECTRUM model 211, cold wall, single wafer CVD tungsten reactor system fully automated computer control as shown in figure 2.1. In this system 10 cm diameter silicon wafers are loaded through a load-lock by a casette-to-casette transport facility. The wafer is positioned against the quartz window in an inverted position and held in place by a lift pins, which leaves the front side exposed to the reactant gases. The wafers are heated on the backside by means of radiant energy through the quartz window, which was generated from a quartz lamb.

The gases used for the experiments are semiconductor-grade tungsten hexafluoride (WF_6) and semiconductor-purity hydrogen (H_2). The WF_6 was provided in an stainless steel container, which was attached to the reactor through a adjust valve. The hydrogen was directly connected with the chamber. The gas flow rate was controlled by the Gas Controller Module in the Spectrum 211. The controllable operation range for mass flow controller are 0-10 sccm (standard cubic centimeters per minute) for tungsten hexafluoride and 0-1000sccm for hydrogen.

Two vacuum pump packages are used in this system. The pump package is a pump system which combined one booster and one rotary vane pump. One pump

pressure at the set point. The second pump package was used to transport the wafer to the chamber. Additional rotary vane pump is used to pump the WF_6 to the air during the ramp and temperature stabilize steps. At these two steps, WF_6 valve is opened to keep the WF_6 flow rate stable.

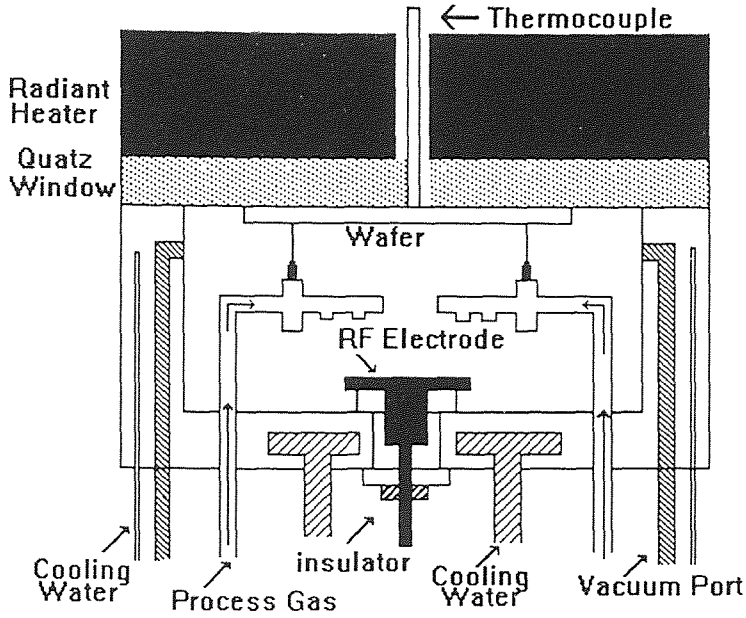

Figure 2.1 Schematic diagram of the chamber

2.1.2 Pre-deposition Preparation

2.1.2.1 Leak Check: A leak check was conducted before beginning of any experimental run to avoid oxygen and ensure formation of films with desirable and reproducible quality. For the SPECTRUM CVD 211, all experimental conditions can be directly read from the monitor; therefore, during this leak check procedure, the champer was

connected to a vacuum system, the pressure decreased to near zero. This process takes several seconds.

2.2 Experimental Procedure

2.2.1 Wafer Preparation and Transport

All wafers were marked first, and weighed accurately to 0.1 mg before and after deposition. In this system 10 cm diameter single crystal, <100> silicon wafers are loaded through a load-lock by a casette-to-cassette transport facility. The whole wafer transport was carried out by automatically control of the machine, and the whole operation process also can be controlled from the monitor.

2.2.2 Film Deposition

The film deposition is achieved in five steps process: (1) pre-purge, (2) ramp up (increasing the reactor temperature rapidly from room temperature to set point), (3) temperature stabilize (time: 30 seconds), (4) tungsten deposition, (5) post purge. The purposes of pre-purge and post-purge are cleaning the chamber. They are divided into several substeps (Table 2). During the ramp and temperature stabilize steps, H_2 is introduced into the chamber and the WF_6 is directly connected with a separate vacuum pump which pumps the WF_6 to the air. In the deposition step, WF_6 is switched to the chamber. The reactor wall were maintained at 30°C by using cooling water at that temperature. During deposition the flow rate, the temperature and the reactor pressure was kept in a small range around the set point.

Table 2 The detailed sub-step in the Pre-purge and Post-purge step

Pre-purge		post-purge	
sub-step	condition	sub-step	condition
1)Purge	P>30mTorr	(1) Pump own	P<10mTorr
2)Pump down	P<10mTorr	(2) Pump own	T=30 second
3)Pump down	T=10 second	(3) Purge	P>30mTorr
4) Purge	P>30 mTorr	(4) Pump down	P<10mTorr
5)Pump down	P<10 mTorr	(5) Pump down	T=30 second
6)Pump down	T=10 second	(6)Purge	P>30 mTorr
		(7) Pump down	P<10mTorr
		(8) Pump down	T=30 second
		(9) Purge	P>30mTorr
		(10)Pump down	P<10mTorr
		(11)Pump down	T=30 second
		(12)Purge	P>30mTorr
		(13)Pump down	P<10mTorr
		(14)Pump down	P>30mTorr

2.3 Tungsten Film Characterization Techniques

2.3.1 Physical Property

2.3.1.1 Film Thickness: The weight change of the wafer after the deposition was measured by electrobalance. Known the wafer area A (78.54 cm^2), and the mass change after deposition, Δm, tungsten film thickness, t, is found from the formula:

$$t = \frac{\Delta m}{\rho_b A} \qquad (2.1)$$

A constant bulk density, ρ_b, of 19.3 g/cm^3 [65] is assumed throughout the calculations.

2.3.2 Structure Property

2.3.2.1 X-ray Diffraction Analysis: The crystallographic orientation of the CVD tungsten film was established by X-ray diffraction measurements using with a Cu target on a Rigaku DMAX II system operating at 30KV and 20mA. Scanning speed of the Goniometer is 2°2θ/min. Tungsten deposited Si wafers are scanned through a 2θ range of 20-90°.

2.3.3 Electrical Property

The sheet resistance values are directly measured by a home-built 4-point probe equipment. The probes are placed colinearly, as shown in figure 2.2 [66]. In this configuration, a constant current I is passed through two of the probes, and the voltage difference between the other two is read. Provided the conducting layer is thin, the sheet resistance can be calculated from the equation

$$R_s = \frac{\pi}{\ln 2}\frac{V}{I} \qquad (2.2)$$

In this experiment, sheet resistivity is measured at different locations on each wafer as shown in figure 2.3. The ranges of voltage and current used in measurements are 1-10 mV and <100 mA, respectively. All the measurements are taken at room temperature.

The film resistivity can be calculated using the resistance. Consider a rectangle of a layer of length l, width b, and thickness t as shown in figure 2.2. The resistance measured in the direction parallel to the film is

$$R_s = \rho \frac{l}{bt} \tag{2.3}$$

where, ρ is the resistivity of the film. If l equal to b, the equation shown as above becomes

$$R_s = \frac{\rho}{t} \tag{2.4}$$

when the thickness and sheet resistance are measured, the film resistivity can be calculated by

$$\rho = R_s t \tag{2.5}$$

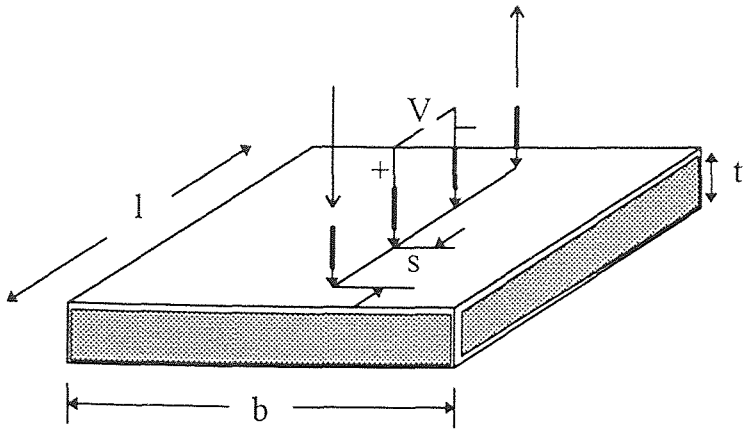

Figure 2.2 Four-point probe system for sheet resistance measurement.

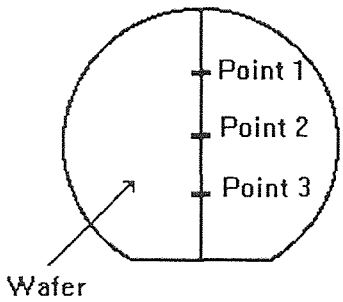

Figure 2.3 The resistivity measurement position on the wafer

2.3.4 Mechanical Property

Film Stress was determined by measuring changes in the radius of curvature of a wafer resulting from deposition on a single side. The distance between two points generated by light from two fixed and paralled He-Ne lasers was determined by reflection from the surface of a wafer before and after deposition. An angled mirror was used to project the

reflection of the two points onto a wall where their separation could be accurately measures. The stress was calculated using Stoney's equation [67]:

$$\sigma=Et_s^2/6(1-\nu)Rt \tag{2.6}$$

where E is Young's modulus for the substrate, ν is Poisson's ratio, t_s is the substrate thickness, t is the film thickness, and the net radius of curvature is

$$R=1(1/R_2-1/R_1) \tag{2.7}$$

where R_1 and R_2 are the radii of curvature of the wafer before and after deposition

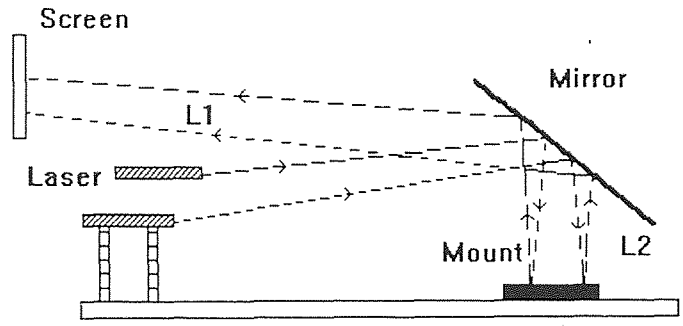

Figure 2.4 Optical system for stress measurement setup

respectively. For Si <100> wafers, $E=1.8\times10^{11}$ Pa and t_s=525 μm. Figure 2.4 shows an optical imaging system for set up.

CHAPTER 3

RESULTS AND DISCUSSION

3.1 The Effects of Deposition Variables on Film Deposition Rate

3.1.1 Temperature Dependent Study

The temperature dependent behavior of deposition rate is shown in Figure 3.1 for the conditions of a constant WF_6 flow rate (5 sccm), H_2 flow rate (100 sccm) and the total reactor pressure (500 mTorr). The figure shows a typical deposition rate vs. temperature dependency for this type of deposition reaction. Two different regimes can be seen which are defined by the rate limiting mechanism of the reaction: (1) The first regime is from 300 °C to 600 °C, the growth rate of tungsten increase quickly with temperature. This regime is controlled by the surface reaction rate.(2) The second regime is above 600 °C. The growth rate of tungsten increase slightly with temperature. This regime is controlled by the rate at which reactant is supplied to the substrate. The reaction rate controlled regime seems to follow an Arrhenius type behavior. An activation energy of about 56 kJ/mol was calculated from the slope in the region where Arrhenius behavior was observed (300-500 °C) by using a linear regression analysis to the following equation:

$$\text{Growth Rate} = k_0 \times e^{\frac{-Ea}{R \cdot T}} \qquad (3.1)$$

This result is comparable to the value 69 kJ/mol reported by Mcconica [43]

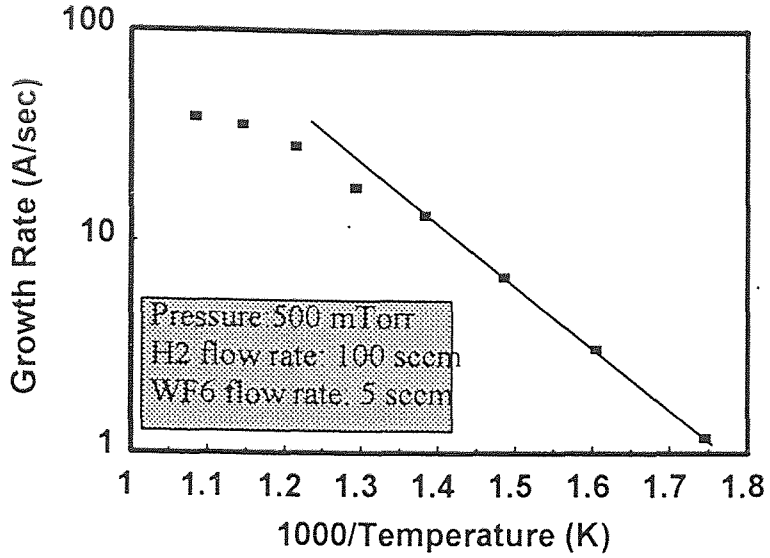

Figure 3.1 Variation of growth rate as a function of temperature at a constant total pressure, WF_6 flow rate, and H_2/WF_6 ratio

3.1.2 Pressure Dependent Study

Under constant conditions of temperature (500 °C), WF_6 flow rate (5 sccm), and H_2/WF_6 ratio (20/1), the pressure dependent behavior of growth rate dependence on pressure was investigated over the range 100 to 1000 mTorr. The results, shown in Figure.3.2, indicate a linear dependence which is consistent with a Langmuir-Hinshelwood mechanism. The higher the pressure, the more gaseous absorbed reactants on the substrate surface, the faster the growth rate. The linear line does not have a zero-pressure intercept caused by the fast Si reduction of WF_6. To obtain the relationship of H_2 partial pressure with the growth rate, first we assume the equilibrium condition to calculate the H_2 partial pressure in the chamber. The quantity of all the species in the chamber are defined as:

$$3H_2 \quad + \quad WF_6 \quad \rightarrow W \quad + \quad 6HF \qquad (3.2)$$

$$F_{H2}\text{-}3X \qquad F_{WF6}\text{-}X \qquad X \qquad 6X \qquad (3.3)$$

F_{H2} and F_{WF6} are the flow rate of H_2 and WF_6 respectively. X is the quantity of WF_6 which is converted to W. Because the reactor was cold wall type and the W selectively deposited on the Si wafer not on the quartz window, we assume all the W are deposited on the Si wafer. So we can use the W growth rate R(cm/sec) and the Si wafer area to calculate X (sccm):

$$X=R\times S_{wafer}\times\rho/M\times 22400\times 60 \qquad (3.4)$$

S_{wafer} is the area of the wafer, which is 78.54 cm^2. ρ is the tungsten density, which is 19.3 g/cm^3. M is the molar weight of tungsten, which is 183.85 g/mol. After calculating the X, the partial pressure of H_2 can be easily calculated:

$$P_{H2}=\frac{F_{H2}-3X}{(F_{H2}-3X)+(F_{WF6}-X)+X+6X}\times P_{total} \qquad (3.5)$$

The relationship of H_2 partial pressure with growth rate is shown in figure 3.3. The diagram shows a linear dependence which is different from other reporter[43,44]. This may be due to the different reactor and different pressure range. Such linear dependence is consistent with a Langmuir-Hinshelwood reaction mechanism. Mcconiica, et al [43]

point out the adsorption of hydrogen is growth rate limited step,. So according to the Langnuir-Hinshelwood mechanism, the growth rate of tungsten for low pressure deposition is given as:

$$Rate=kKP_{H2}/(1+KP_{H2}) \qquad (3.6)$$

Where k is the reaction rate constant and K is the adsorption equilibrium constant. For low pressure values, KP_{H2} is small compared to 1 thus yielding the observed linear dependence.

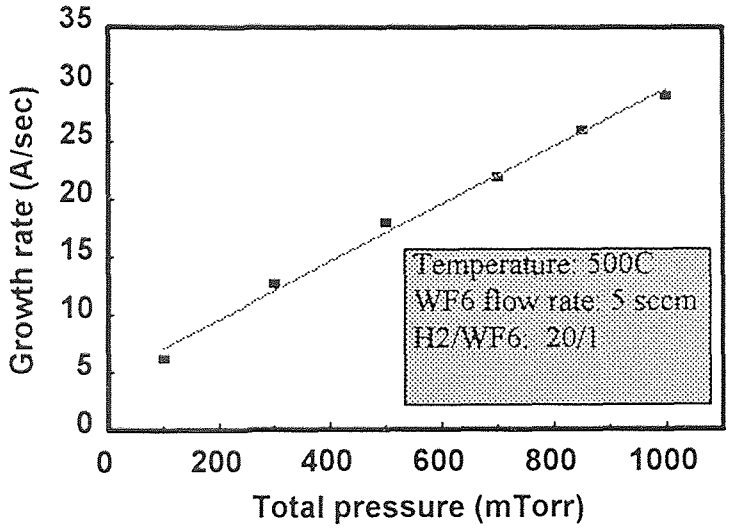

Figure 3.2 Variation of growth rate as a function of total pressure at a constant temperature, WF_6 flow rate, and H_2/WF_6 ratio

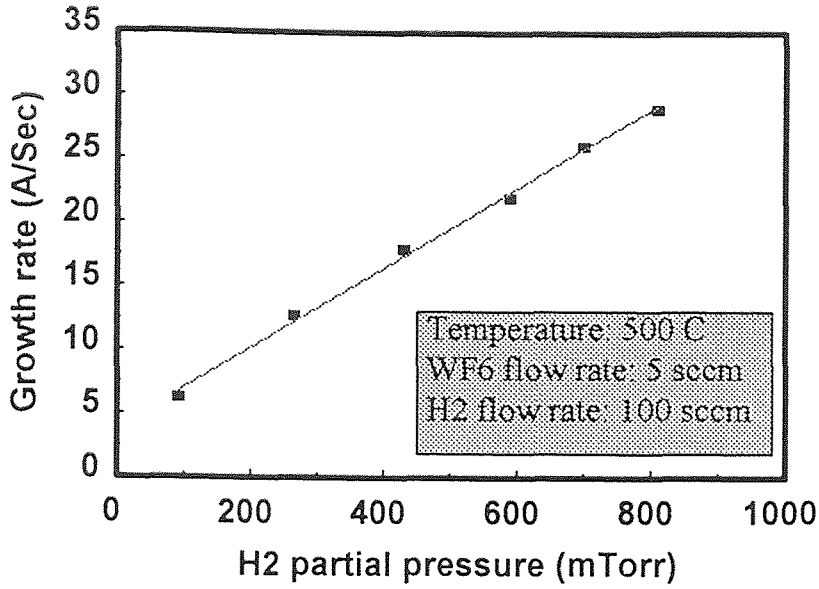

Figure 3.3 Variation of growth rate as a function of H_2 partial pressure at a constant temperature and WF_6 flow rate, and H_2/WF_6 ratio

3.1.3 Flow Ratio Dependent Study

In Figure.3.4, the deposition rate is plotted as a function of H_2/WF_6 ratio for constant conditions of growth temperature (500°C), total pressure (500mTorr) and WF_6 flow rate (5sccm). The deposition rate was found to increase in the low flow ratio regime (below 10) followed by saturation above this flow ratio. The former H_2 partial pressure effect on growth rate study show that the deposition rate increase with the partial pressure of H_2. Therefore, when the flow ratio (H_2/WF_6) increase, the partial pressure of H_2 increase, the deposition rate increase. But after the flow ratio reach a certain value, the H_2 in the chamber will saturate and not enough WF_6 is present to meet the increasement of deposition rate. The deposition rate will no longer increase.

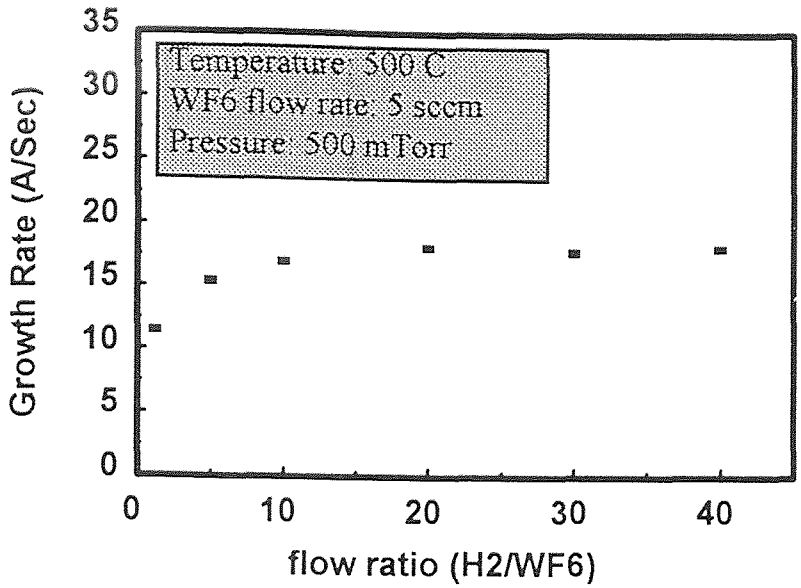

Figure 3.4 Variation of growth rate as a function of flow ratio at a constant temperature, pressure and WF_6 flow rate

3.2 Tungsten Film Characteristics

3.2.1 Stress

The stress of the deposited film is a very important aspect of tungsten film for X-ray absorber application and as interconnect material. Stress in the absorber exerts a torque on the membrane at the edges of features, and this leads to out-of-plane and in plane distortion. In order to find the effect of deposition condition on film stress, three operation parameters are considered to be variables for the stress studies. The three studies are based on the standard reaction condition (growth temperature 500°C, total pressure 500 mTorr, the flow ratio of H_2 to WF_6 20). The ranges for these parameters were varied from 300-625°C for the temperature series, from 100 to 1000 mTorr for

pressure series and from 1 to 40 for flow ratio series. These results are shown in Figure 3.5, 3.6 and 3.7 respectively.

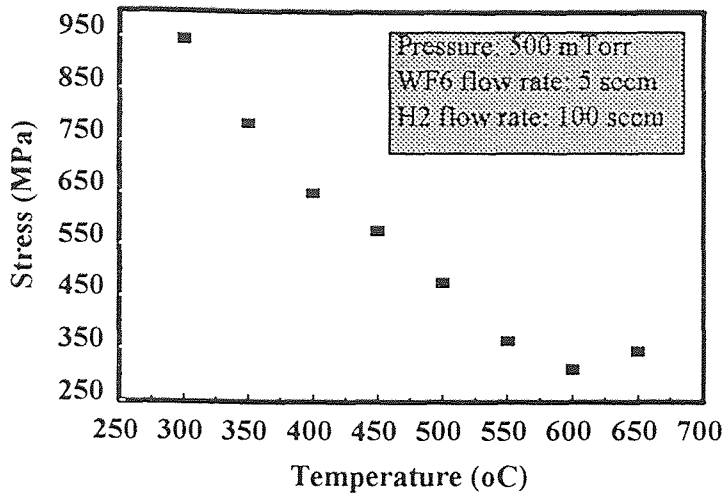

Figure 3.5 Variation of stress as a function of temperature at a constant pressure, WF_6 flow rate, and H_2/WF_6 ratio.

3.2.1.1 Temperature effect: It is clear the stress in the tungsten film has a strong relationship with temperature. Between the 300 and 600°C, the stress decrease largely with temperature. According to the buried layer (BL) model for steady-state film growth proposed by Klokholm and Berry[68], it is suggested that tensile growth stresses are generated " by the annealing and constrained shrinkage of disordered material buried behind the advancing surface of the growing film." It is assumed that the amount of built-in disorder is proportional to the final stress in the film after complete relaxation. The model predicts that the tensile growth stress increases with increasing growth rates and/or decreasing deposition temperatures.

The measured tensile growth stress at approximately 7000Å thickness can be analyzed using the concepts of Klokholm and Berry. An activated surface relaxation process is defined with atomic jump frequency ν:

$$\nu=\nu_o\exp(-Es/RT) \tag{3.7}$$

with ν_o a frequency factor, Es an activation energy, R the gas constant, and T the absolute substrate temperature. The number of jumps n_j a surface atom can make before it is buried behind the growing surface will then approximately be

$$n_j\approx\nu r^{-1} \tag{3.8}$$

with r the growth rate in monolayers (ml) per second. If this number of jumps is low, lattice defects will be present in an as-deposited incremental layer of the film. These defects represent an excess volume ΔVm, which, due to relaxation, will be transformed to an elastic strain in the film. The excess volume is defined as the difference between the molar volume of the as deposited, unrelaxed film and the molar volume Vm of a relaxed constrained film. If we assume this excess volume to be proportional to n_j^{-1}, then

$$\frac{1}{3}\frac{\Delta V_m}{V_m}=\varepsilon=\sigma\frac{1-\nu_f}{E_f}=kn_j^{-1}=kr\nu^{-1} \tag{3.9}$$

or

$$\ln\frac{\varepsilon}{r} = \ln\frac{k}{\nu_o} + \frac{E_s}{RT} \tag{3.10}$$

where ε is the biaxial strain, σ is the biaxial stress, and k is a proportionality factor. Assuming the tungsten film's modulus (E_f= 410 GPa) is not dependent on the deposition temperature and is almost elastically isotropic (ν_f=0.28), so 1 GPa biaxial stress corresponds to 0.18% biaxial strain. According to Equation 9 the strain increases linearly with the growth rate, while it decreases exponentially with the deposition temperature. If the above mentioned model is valid, the logarithm of εr^{-1}, as determined from the σ values, versus the reciprocal absolute temperature should yield a straight line. Taking the thickness of a W monolayer, 2.74 Å, a straight line is obtained, with a slope corresponding to 59 kJ/mol .This value is different from the value 143 kJ/mol reported by Leusink et al. [69].

After temperature is higher than 600°C, stress increase slightly. This may be due to the strong substrate encroachment. The higher the temperature, the more the silicon consumption problem. Kamins, et al.[70] concluded that a significant contribution to the stress can arise from the initial reaction between the WF_6 and Si and little intrinsic stress is added during the hydrogen reduction reaction. The high substrate encroachment lead to the higher stress. Another Reason is that the reaction is in the mass-transport limited regime, the film always has sufficient time to complete relaxation before buried by the advancing surface of the growing film. So the stress no longer has relationship with the

temperature. This suggest Es in the buried layer model is only applicable in the reaction rate limited regime.

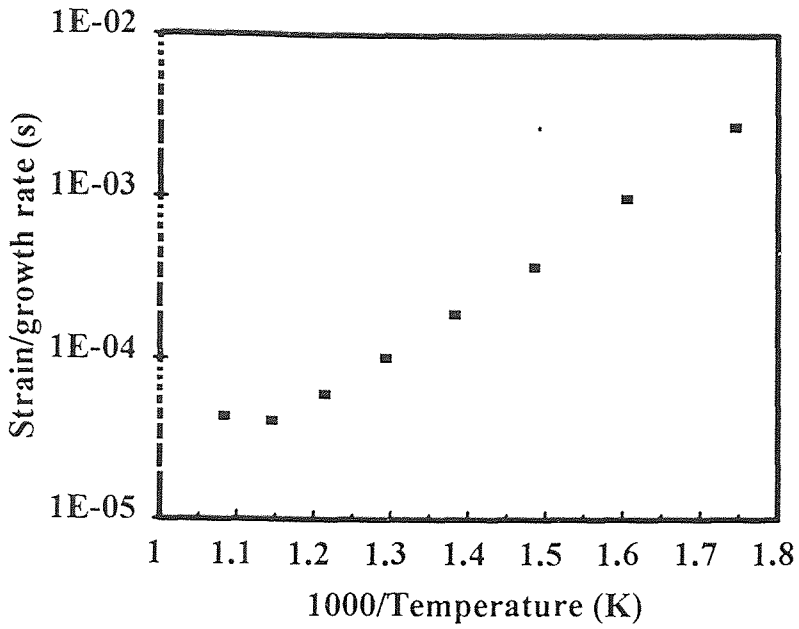

Figure 3.6 Variation of εr^{-1} as a function of reciprocal temperature

3.2.1.2 Pressure Effect: The pressure dependent behavior of stress is shown in figure 3.7, with the condition of a constant temperature (500 °C) and flow ratio 20. The stress increase with the pressure. When the pressure increase, the deposition rate increase. From the buried layer (BL) model, We know the stress in the film is linearly with the deposition rate. So the pressure increase, the stress increase. But compared with the temperature effect, the pressure effect is not very strong.

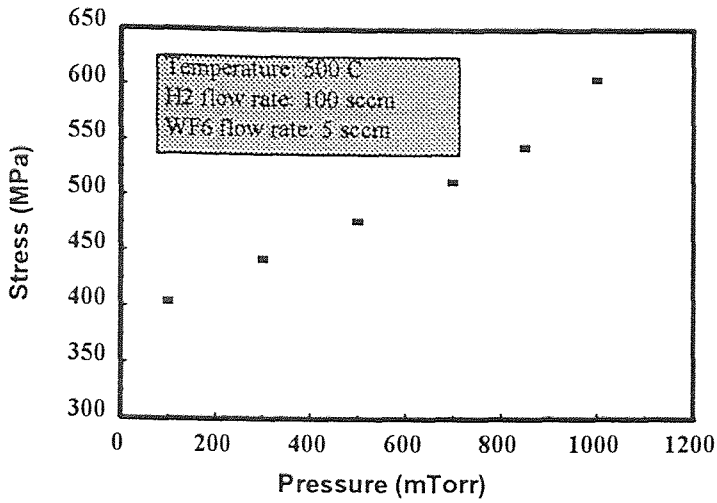

Figure 3.7 Variation of stress as a function of pressure at a constant temperature, WF6 flow rate, and H_2/WF_6 ratio

3.2.1.3 Flow Ratio Effect: The flow ratio effect on the film stress was studied on the constant WF_6 flow rate 5 sccm, temperature 500 °C, and pressure 500 mTorr. Before the ratio reach to 10, the stress increases quickly due to the deposition rate increase. After this ratio, the stress tend to keep as constant. From the kinetics study, we know the H_2 in the reaction chamber saturate at the high flow ratio and the stress no longer increase because of the constant deposition rate.

3.2.2 Resistivity

Another important application of the tungsten film is for interconnect material. The primary requirements for the interconnect material are low resistivity. This low resistivity can allow higher current density to be imposed on tungsten wiring with a

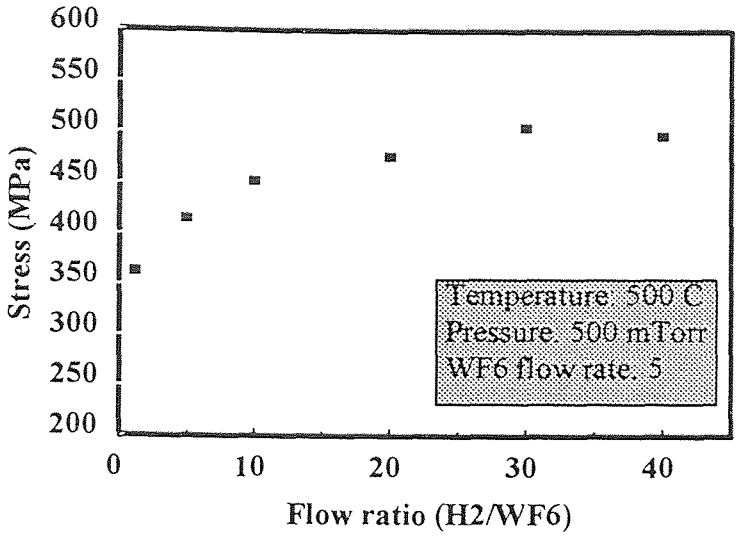

Figure 3.8 Variation of stress as a function of flow ratio at constant temperature, pressure and WF_6 flow rate

smaller line width, minimized interconnection or RC time delay of the device. Deposited tungsten film resistivites were calculated from sheet resistance values and film thickness. The film thickness values used were those calculated from the gravimetric, constant density analysis, for which a constant film density (19.3 g/cm^3) was assumed. In fact, the density of deposited tungsten film maybe is different from the bulk density. An accurate film thickness shoud be measured from SEM, stylus profilometer, etc[71]. Reported values for resistivities correspond to the measurement values. The resistivities were found to be higher than tungsten bulk resistivity, 5.3 μΩ-cm at 20 °C [33].

In order to investigate the resistivity further, three operation parameters (temperature, pressure and flow ratio) are considered as variables for the resistivity

studies. The three studies are based on the same condition as these parameters effect on stress study. These results are shown from figure 3.9 to figure 3.11 , and it is clear that the measured resistivity varies in a small range for both pressure and flow rate study series. The independent behaviors of pressure (100-1000 mTorr) series and flow rate (1 to 40) series can be determined. However, in temperature study series, shown in figure 3.9, the values of resistivity seems to increase at the lower deposition temperature from 350 to 300°C and decrease at the higher temperature. When W deposited at the lower temperature, the poorly connected grains of structure, and the electron scattering effect caused by phonons, impurities, vacancies, dislocations, grain boundaries, precipitated second phase particles, and compound phase [72] may be used as an explanations for low resistivity at low temperature. when deposited at high temperature, the grain size is large[54], this will result in the resistivity decreasing.

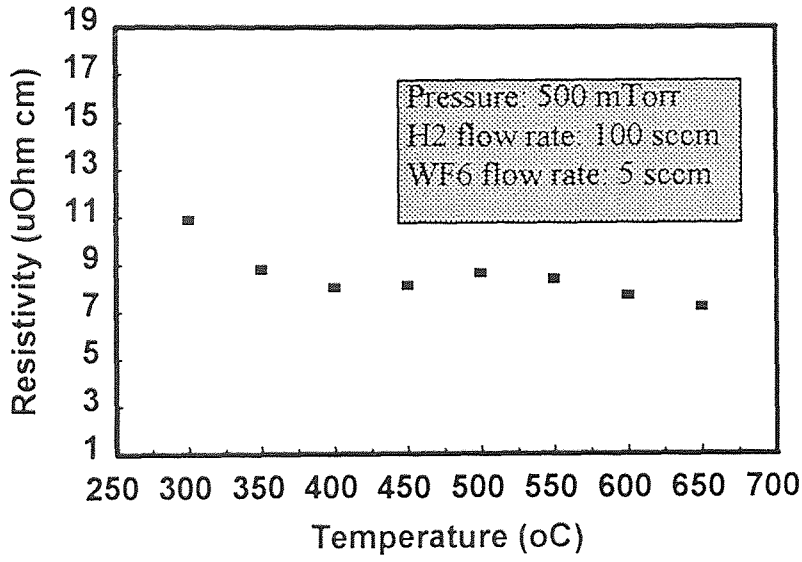

Figure 3.9 The dependent behavior of resistivity of CVD W on temperature

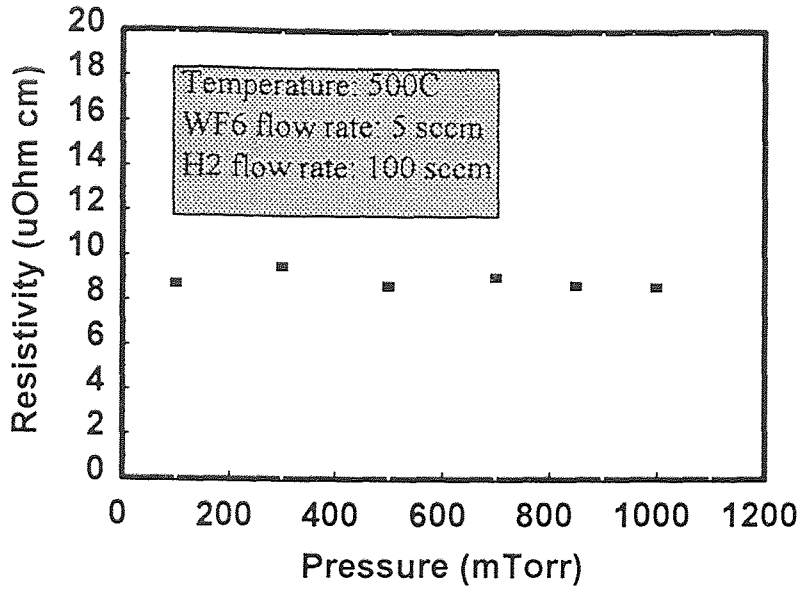

Figure 3.10 The independent behavior of resistivity of CVD W on total pressure

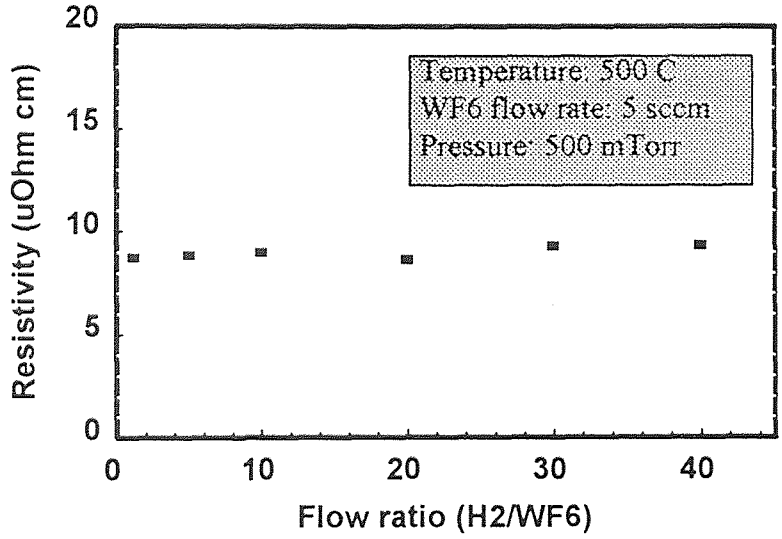

Figure 3.11 The independent behavior of resistivity of CVD W on flow ratio

3.2.3 Crystal Orientation

The types of phase and orientation of tungsten crystals formed by the deposition reaction were examined by X-ray diffraction analysis. The range examined for 2θ was between 30° and 80°, wide enough to identify α-W, β-W, and tungsten silicide phase. All the temperature series, pressure series and flow ratio series were measured by X-ray diffraction. No film was found to contain trace amount of β-W, whose characteristic peaks exist on 35.6, 40.04, 43.91, 64.17, 66.76, 70.17, 75.37 2θ° [73]. Figure 3.12 shows the typical X-ray diffraction pattern of tungsten film. Three α-tungsten charateristical peaks (40.26, 58.27, and 73.19 2θ,°) corresponding to lattice spacing (2.238, 1.582, 1.292 Å) are apparent in all the diffraction pattern.

The preferred orientation of the specific (hkl) plane can be evaluated by texture coefficient, TC (hkl) [74]:

$$TC(hkl) = \frac{\mathrm{Im}(hkl)}{I_r(hkl)} \Big/ \frac{1}{n}\sum_{i=1}^{n}\frac{\mathrm{Im}(hkl)}{I_r(hkl)} \qquad (3.11)$$

where I_m (hkl) is the measured X-ray relative intensity of the (hkl) plane, I_r (hkl) is the relative intensity in the powder pattern, and n is the total number of reflection peaks. Table 4 give the X-ray relative intensity of tungsten random powder[73].

The larger TC values mean a more markable orientation. If TC (hkl) is less than 1, the (hkl) plane has no preferred orientation. All the samples'TC (110) and TC (211) are less than 1 and TC (200) are larger than 1, so there is preferred orientation (200).

This is because the W (200) plane has same in-plane lattice geometry of square as the Si (100) plane, however, the W (110) has diamond in-plane lattice geometry[65]. The anothert reason is that the bcc tungsten is not closed packed and more open compared with (110) plane, the tungsten may be easy to adsorb on this open structure.

Figure 3.13 depicts the effect of deposition temperature on preferred orientation of (200). Between 300 to 400 °C, the preferred orientation of (200) increase with the temperature, then decrease quickly up to 500°C, after this the preferred orientation increase again. The temperature change will affect the adsorbate surface diffusion on the (200) and (110) plane, will affect the reconstruction of (200) plane [75], and will change the interface of Si/W. These factors all will affect the orientation of the films. It is these factors' inter balance that lead to this unique trend. R. Blumenthal, et al.[54] observed another phenomenon, the amount of (200) orientation decreases from 400-450°C, peaks at 500°C, and disappears as the temperature increases up to 650°C. This different result may be due to the different substrate. They coated Si wafer with SiO_2 and TiW layer. It is known the lattice match between the substrate and the growing film will determine the crystal orientation.

The pressure effect on the texture coefficient of (200) plane is shown on Figure 3.14. The preferred orientation of (200) plane increase with pressure followed by a constant trend. But this trend is not remarkable compared with that of the temperature dependency because the TC (200) kept in a small range between 1.4 to 1.6.

The flow ratio has a strong relationship with TC (200) which is shown on Figure 3.15. The preferred orientation of (200) plane decrease quickly with flow ratio than tend

to keep as constant at high flow ratio. This relationship is exactly opposite to the relationship between flow ratio and growth rate. We can not attribute the effect of flow ratio on TC (200) behavior to deposition rate because in the pressure series we find the opposite trend is formed. The reason which lead to this behavior is that more hydrogen which occupy the sites on the tungsten (200) plane will prevent the W adsorbing on this plane, then (200) plane orientation will decrease.

Table 4. X-ray diffraction lines for α-W from random tungsten powder

plane	lattice spacing (Å)	relative intensity	2θ
110	2.238	100	40.26
200	1.582	15	58.27
211	1.292	23	73.19

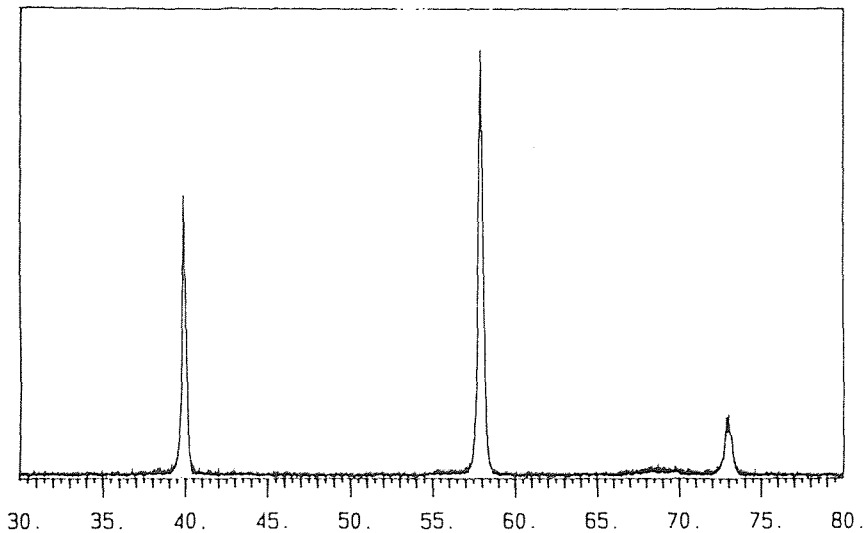

Figure 3.12 The typical X-ray diffraction of tungsten film

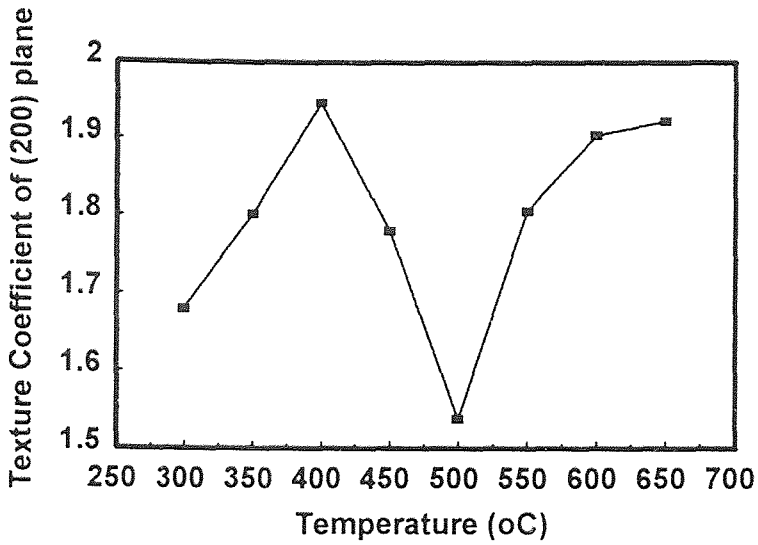

Figure 3.13 Temperature effect on texture coefficient of (200) plane

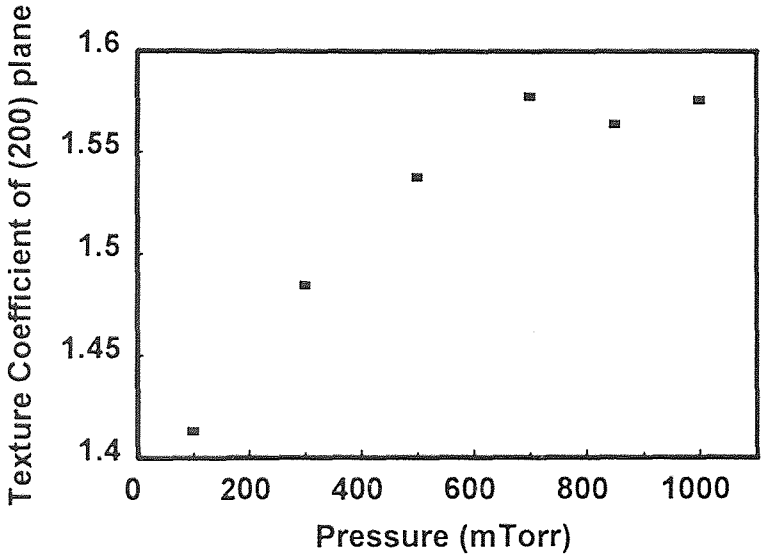

Figure 3.14 Pressure effect on texture coefficient of (200) plane

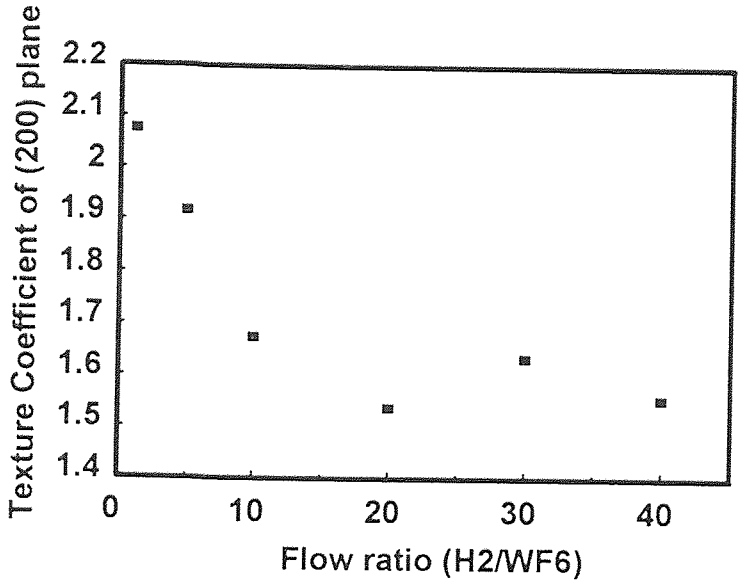

Figure 3.15 Flow ratio effect on texture coefficient of (200) plane

CHAPTER 4

CONCLUSIONS AND SUGGESTIONS

This research included the fabrication and characterization of CVD tungsten film from H_2 and WF_6 for X-ray absorber in X-ray lithography technology.

Low stress films have successfully been synthesized on pure silicon wafers in a cold wall, single wafer reactor by low pressure chemical vapor deposition from H_2 and WF_6 in the temperature range of 300-650 °C, pressure range of 100-1000 mTorr, flow ratio range of 1-40. The growth kinetics were determined as a function of temperature, pressure and flow ratio. The deposition rate as deposited films was found to follow an Arrehnius behavior in the range of 300-500°C with an activation energy of 55.7 kJ/mol. The growth rate was seen to increase linearly with total pressure and H_2 partial pressure. In the H_2/WF_6 flow ratio studies conducted at 500°C and 500 mTorr, growth rate increase with flow ratio when flow ratio is lower than 10 followed by saturation above this ratio. The stress of deposited film strongly dependent on temperature and has weak relationship with pressure and flow ratio. These three parameters effect on stress can be explained by buried layer model which show the stress of as deposited film linearly dependent on growth rate factor and exponentially dependent on temperature factor. Low resistivity values (less than 10 $\mu\Omega \cdot$ cm) were obtained for as-deposited condition. The pressure and flow ratio seem no effect on resistivity but resistivity is lower at high temperature and higher temperature. The X-ray diffraction patterns indicate the

<200> has preferred orientation in all as deposited films. The preferred orientation increase with temperature from 300 to 400 °C, then decrease up to 500°C, then increase again. The preferred orientation increase with pressure followed by constant at high pressure. But the preferred orientation decrease with flow ratio then tend to keep at constant at high flow ratio.

However, this study still did not synthesize free stress film. Some improvement must be done which include:

(1) Wafer treatment:

Some researches show the major stress in the CVD tungsten film come from the reaction interface of W/Si, So preventing the reaction in the interface between Si and W can reduce the stress. This can be realized by first depositing TiN at the Si wafer. This TiN layer not only can reduce the stress but also can improve the W adhesion to the substrate.

We deposit the W on the Si wafer, but Si is not a good material for X-ray mask membrane. We had better deposit W on the SiC or SiN substrate. Because the different substrate will lead to different nucleation it is expected to obtain the different optional W deposition condition.

(2) Plasma CVD process conditions:

Plasma enhanced chemical vapor deposition of W can get the compressive stress but low pressure chemical vapor deposition of W can get the tensile stress. If we can combine these two processes, maybe we can get the free stress film.

(3) Reduction agent development:

There are several chemicals which can be used to reduce WF_6 precursor. Silane is one of the candidates in that it will suppress the reaction between W and Si. We should explore the stress if plasma-enhanced deposited from the silane using Spectrum 211.

(4) Anneal as deposited film

Annealing the as deposited film will decrease the stress in the film. We should try to use the method and find the mechanism of this method.

REFERENCES

1. A.Heuberger, *J.Vac.Sci.Technol.*, **B6(1)**, 107 (1988).

2. R.A.Colclaser, *Microelectronics:Processing and Design.*, J.Wiley and Sons, Inc., New York, (1980).

3. Alan.D.Wilson, *SPIE 537, Electron-Beam, X-Ray, and Ion-Beam Techniques for Submicrometer Lithographies IV.*, 85 (1985).

4. A.Heuberger, *Solid Sstate Technology.*, **2**, 93 (1986).

5. A.R.Shimkunas, *Solid State Technology.*, **9**, 192 (1984).

6. Aubrey Tobey, *Microelectronic Manufacturing and Testing.*, **6**, 35 (1987).

7. A.W.Yanof, D.J.Resnick, C.A. Jankoski, and W.A.Johnson, *Proceedings of the SPIE.*, Santa Clara, CA, edited by P.D.Blais, 632 (1986).

8. H.Betz, H.-l.Huber, S. Pongratz, W.Rohrmoser, and W. Windbracke, *Microelectron. Eng.*, **5**, 41 (1986).

9. I.Plotnik, M.E.Porter, M.Toth, S.Akhtar, and Henry I. Smith, *Microelectronic Engineering.*, **5**, 51 (1986).

10. M.Karnezos, R.Ruby, B.Heflinger, H.Nakano, and R.Jones, *J.Vac.Sci.Technol.*, **B5**, 283 (1987).

11. A.M.Gosnet and F.R.Ladan, *Microelectron Eng.*, **6**, 253 (1987).

12. Yao C. Ku and Henryl. Smith, *J.Vac.Sci.Technol.*, **B6(6)**, 2174 (1988).

13. H.Luethje, M.Harms, A. Bruns,and V.Mackens, *Microelectron. Eng.*, **6**, 259 (1987).

14. Nobuyuki Yoshioka, Susumu Takeuchi, Hiroaki Morimoto and Yaichiro Watakabe, *SPIE, Electron-Beam X-ray, and Ion-beam Technology. Submicrometer Lithographies VII.*, 923 (1988).

15. Kern, W. Chemical Vapor Deposition. R.A.Levy Eds., *Microelectronic Materials and Processes.*, Kluwar Academic, New Jersey, 203 (1986).

16. D.W.Shaw, *Crystal Growth*, C.H.L.Goodman Eds, Plenum Press, London, 1, (1974).

17. S.Wolf and R.N.Tauber, *Silicon Processing for the VLSI Era.*, Lattice Press, California, 110 (1986).

18. Laidler, K.J, *Chemical Kinetics.*, Harper & Row, New York, 267 (1987).

19. A.W.Vere, *Crystal Growth Principles and Progress.*, Plenum Press, New York,

20. A.Reisman and M.Berkenblit, *J.Electrochem. Soc.*, **113**, 146 (1966).

21. S.Wolf and R.N.Tauber, *Silicon Processing for the VLSI Era.*, Lattice Press, California, 124 (1986).

22. H.C.Theurer, *J.Electrochem. Soc.*, **108**, 649 (1961).

23. W.Kern and V.S.Ban, *Thin Film Processes.*, J.L.Vossen and W.Kern, Eds., Academic Press, New York, (1978).

24. W.Kern and G.L.Schnable, *IEEE Trans.Electron Devices.*, **ED-26**, 647 (1979).

25. R.S.Rosler, *Solid State Technol.*, **20(4)**, 63 (1977).

26. A.R.Reinberg, *Annu.Rev. Mater.Sci.*, **9**, 341 (1979).

27. T.Sugano, *Application of Plasma Processes to VLSI Technology.*, John Wiley & Sons, New York ,(1985).

28. J.W.Peters, F.L.Gebhart, and T.C.Hall, *Solid State Technol.*, **23(9)**, 121 (1980).

29. J.W.Peters, *IEEE-IEDM Tech.Dig.*, 240 (1981).

30. S.D.Allen, A.B.Trigubo, and Y.-C.Liu, Chemical Vapor Deposition, J.M.Blocher, Jr., G.E.Vuillard, and G.Wahl, Eds., *The Electrochemical Society.*, Pennington, New Jersey, 267 (1981).

31. Y.Kusumoto, K.Takakuwa, H.Hashinokuchi, T.Ikuta, and I.Nakayama, *Tungsten and Other Refractory Metals for VLSI Applications III.*, V.A.Wells, Ed.,MRS Publishers, Pittsburg, Pennsylvania, 3 (1988).

32. J.Randall Creighton, and John E.Parmeter, *Critical Reviews in solid State and Materials Sciences.*, **18(2),** 175, (1993).

33. R.A.Levy, and M.L.Green, *J.Electrochem. Soc.*,**134(2)**, 37 (1987).

34. M.Diem, M.Fisk, and J.Goldman, *Thin Solid Films.*, **107**, 39 (1983).

35. Y.Kusumoto, K.Takakuwa, H.Hashinokuchi, T.Ikuta and I.Nakayama, *Tungsten and Other Refractory Metals for VLSI Applications III.*, V.A.Wells, Ed., MRS Publishers, Pittsburg, Pennsylvania, 103 (1988).

36. Mehrdad M.Moslehi, *ibid*, 385.

37. E.K.Broadbent, and C.L.Ramiller, *J.Electrochem.Soc.*, **131**, 1427 (1984).

38. N.Lifshitz, *Tungsten and Other Refractory Metals for VLSI Applications III.*, V.A.Wells, Ed., MRS Publishers, Pittsburg, Pennsylvania, 83 (1988).

39. M.L. Green, Y.S.Ali, T.Boone, B.A. Davidson, L.C.Feldman, and S.Nakagara, Tungsten and Other Refractory Metals for VLSI Application II., E.K.Broadbent, Ed., MRS Publishers, Pittsburg, Pennsylvania, 85, (1986).

40. M.E.Tracy, *Tungsten and other Refractory Metals for VLSI Applications.*, R.S.Blewer, Editors., MRS Publishers, Pittsburg, Pennsylvania, (1985).

41. R.V.Joshi, D.A.Smith, S.Basavaiah, and T.Lin, *Tungsten and Other Refractory Metals for VLSI Applications III.*, V.A.Wells, Ed., MRS Publishers, Pittsburg, Pennsylvania, 39 (1988).

42. K.Y.Tsao and H.H.Busta, *J Electrochem. Soc.*, **131**, 2702 (1984).

43. C.M.MCConica and K.Krishnamani, *J Electrochem.Soc.*, **133**, 2542 (1986).

44. E.K.Broadbent and C.L.Ramiller, *J.Electrochem.Soc.*, **131**, 1427 (1984).

45. R.V.Joshi, D.A.Smith, S.Basavaiah, and T.Lin, *Tungsten and other Refractory Meatls for VLSI Applications.*, R.S.Blewer, Editors, MRS Publishers, Pittsburg, Pennsylvania, 39,(1985).

46. J.R.Creighton, *J.Vac.Sci. Technol.*, **A7**, 621 (1989).

47. A.M.Shroff and G.Delval, *High Temperatures-high Pressures.*, **3**, 695 (1971).

48. R.A. Levy and M.L.Green, *Mat. Res.Soc.Symp.Proc.*, **71**, 229 (1986).

49. M.R.McLaury, R.W.Stoll, and D.W.Woodruff, *Tungsten and other Refractory Meatls for VLSI Applications.*, R.S.Blewer, Editors, MRS Publishers, Pittsburg, Pennsylvania, 467 (1985).

50. W.T.Stacy, E.K.Broadbent, and M.H.Norcott, *J. Electrochem. Soc.*, **131**, 444 (1985).

51. J.Weissman and M.C.Kinter, *J.Am.Phys.Soc.*, **34**, 3187 (1963).

52. T.I.Kamins, D.R.Bradbury, T.R.Cass, S.S.Laderman, and G.A.Reid, *J.Electrochem. Soc.*, **133**, 2555 (1986).

53. R.V.Joshi, E.Mehter, M.Chow, M.Ishaq, S.Kang, P.Geraghty, J.Mclnerney, *Tungsten and Other Advanced Metals for VLSI/ULSI Applications V.*, S.S.Wong and S. Furukawa, Eds, MRS Publishers, Pittsburg, Pennsylvania, 157 (1990).

54. R.Blumenthal, G.C.Smith, H.Y.Liu and H.L.Tsai, *ibid.*, 65.

55. T.Ohba, T.Suzuki, T.Hara, Y.Furumura, and K.Wada, *ibid.*, 17.

56. J.E.J. Schmitz, A.J.M. van Dijk, and M.W.M. Graef, *Proc. Of the 10th Int. Conf. On CVD.*, G.W.Cullen, Ed, Electrochem. Soc., Princeton, New Jersey, **87**, 625

57. N.Kobayashi, H.Goto, and M.Suzuki, *Proc. of 11th International Conf. CVD.*, Electrochem. Soc., Princeton, New Jersey, 434 (1990).

58. C.A.Van der Jeugd, A.H.Verbruggen, G.J.Leusink, G.C.A.M.Janssen, and S.Radehar, *Tungstenand Other Advanced Metals for VLSI/ULSI Applications V.*, S.S.Wong and S. Furukawa, Eds, MRS Publishers, Pittsburg, Pennsylvania, 267 (1990).

59. M.Suzuki, N.Kobayashi, and K.Mukai, *ibid.*, 259.

60. S.Sivaram, M.L.A.Dass, C.S.Wei, B.Tracy, and R.Shukla, *J.Vac.Sci.Technol.*, **A11(1)**, 87, (1993).

61. J.E.J.Schmitz, A.J.M. Van Dijk, and M.W.M.Graef, *Proc. Of the 10th Int. Conf. On CVD.*, G.W.Cullen, Ed, Electrochem. Soc., Princeton, New Jersey, **87**, 625

62. M.Saitoh, T.Nishoida, M.Suzuki, N.Kobayashi, and T.Kure, *Tungsten and Other Advanced Metals for VLSI/ULSI Applications V.*, S.S.Wong and S. Furukawa, Eds, MRS Publishers, Pittsburg, Pennsylvania, 201 (1990).

63. Takayuki Ohba and Shin-ichi Inoue, *ibid.*, 281.

64. Takashi Akahori, Takayuki Tani, and Satoshi Nakayama, *Tungstenand Other Advanced Metals for VLSI/ULSI Applications V.*, S.S.Wong and S. Furukawa, Eds, MRS Publishers, Pittsburg, Pennsylvania, 209 (1990).

65. Oktay H.Gokce, Ph.D. Thesis, *Kinetics of the Tungsten Hexafluorine-Silane Reaction for the Chemical Vapor Deposition of Tungsten.*, Montana State University, Bozeman, Montana (1991).

66. L.I. Maissel, *Handbook of Thin Film Technology.*, L.I.Maissel and R.Glang, Eds McGraw-Hill, New York, 1, (1970).

67. Stoney, G.G. *Proc.R.Soc.*, London, **A82**, 172 (1909).

68. E.Klokholm and B.S.Berry, *J.Electrochem.Soc.*, **115**, 823 (1968).

69. G.J.Leusink, T.G.M.Oosterlaken, G.C.A.M.Janssen, and S.Radelaar, *J. Appl. Phys.*, **(6)**, 3899, (1993)

70. T.I.Kamins, D.R.Bradbury, T.R.Cass, S.S.Laderman, and G.A.Reid, *J.Electrochem. Soc.*, **133(12)**, 2555 (1987).

71. Milton Ohring, *The Materials Science of Thin Films.*, Academic Press, Inc. San Diego, California (1992)

72. Do-Heyoung Kim, Robert H.Wentorf, and William N.Gill, *J.Electrochem.Soc.*, 3273 (1993).

73. *X-ray Powder Data File.*, J.V. Smith, Ed., American Society for Testing and Materials, Philadelphia, (1960).

74. M.S.Kim and J.S.Chun, *Thin Solid Films.*, **107**, 29 (1983).

75. J.M.MacLaren, J.B. Pendry, P.J.Rous, D.K.Saldin, G.A.Somorjai, M.A.Van Hove, and D.D.Vvendensky, Surface Crystallographic Information Service. Handkook of Surface Structures., D.Reidel Publishing Company, Dordrecht, Holland (1988)